CHAOS AND SYNCHRONY IN A MODEL OF A HYPERCOLUMN IN VISUAL CORTEX

D. Hansel

Centre de Physique Théorique
UPR014-CNRS, Ecole Polytechnique, 91128 Palaiseau, France
E-mail: hansel@orphee.polytechnique.fr

and

H. Sompolinsky

Racah Institute of Physics and Center for Neural Computation
The Hebrew University, Jerusalem, Israel 91904
E-mail: haim@fiz.huji.ac.il

ABSTRACT

Neurons in cortical slices emit spikes or bursts of spikes regularly in response to a suprathreshold current injection. This behavior is in marked contrast to the behavior of cortical neurons in-vivo, whose response to electrical or sensory input displays a strong degree of irregularity. Correlation measurements show significant degree of synchrony in the temporal fluctuations of neuronal activities in cortex. We explore the hypothesis that these phenomena are the result of the synchronized chaos generated by the deterministic dynamics of local cortical networks. A model of a "hypercolumn" in the visual cortex is studied. It consists of two populations of neurons, one inhibitory and one excitatory. The dynamics of the neurons is based on a Hodgkin-Huxley type model of excitable voltage-clamped cells with several cellular and synaptic conductances. A slow potassium current is included in the dynamics of the excitatory population to reproduce the observed adaptation of the spike trains emitted by these neurons. The pattern of connectivity has a spatial structure which is correlated with the internal organization of hypercolumns in orientation columns. Numerical simulations of the model show that in an appropriate parameter range, the network settles in a synchronous chaotic state, characterized by a strong temporal variability of the neural activity which is correlated across the hypercolumn. Strong inhibitory feedback is essential for the stabilization of this state. These results show that the cooperative dynamics of large neuronal networks are capable of generating variability and synchrony similar to those observed in cortex. Auto-correlation and cross-correlation functions of neuronal spike trains are computed, and their temporal and spatial features are analyzed. In other parameter regimes, the network exhibits two additional states: synchronized oscillations and asynchronous state. We use our model to study cortical mechanisms for orientation selectivity. It is shown that in a suitable parameter regime, when the input is not oriented, the network has a continuum of states, each representing an inhomogeneous population activity which is peaked at one of the orientation columns. As a result, when a weakly oriented input stimulates the network, it yields a sharp orientation tuning. The properties of the network in this regime, including the appearance of *virtual rotations* and broad stimulus-dependent cross-correlations, are investigated. The results agree with the predictions of the mean field theory which was previously derived for a simplified model of stochastic, two-state neurons. The relation between the results of the model and experiments in visual cortex are discussed.

1. Introduction

1.1. Variability and synchrony in cortex

This paper addresses two ubiquitous characteristics of neuronal dynamics in cortex. One is the strong degree of irregularity in the responses of cortical neurons. The spikes emitted by the same neurons *in vivo* have stochastic features, with inter-spike histograms which often resemble that of a Poisson process [1]-[6]. Furthermore, the response patterns show a large degree of variability upon repetition of the same electrical or sensory stimulation. This behavior is in marked contrast to the behavior of the same types of neurons in cortical slices. When a constant current larger than a threshold value is injected into cells *in vitro*, most of them exhibit regular responses which take the form of trains of single spikes or trains of bursts of spikes with a frequency which is either constant in time or decreases due to adaptation [7]. Furthermore, the response pattern of a cell is highly reproducible under repetition of the electrical stimulation. At present, the mechanism generating the irregularity in neuronal actions in cortex is not well understood [8, 9].

A second feature of cortical dynamics is the synchrony in the responses of neurons even when they are far apart [10]-[14]. This synchrony can be observed by several means. The temporal fluctuations of local field potentials measure indirectly the coherence in local groups of neurons. Direct measurements of synchrony is provided by cross-correlation (CC) functions of spike trains of pairs of neurons, or CCs of local field potentials at different sites. In most of the cases, these CCs do not show a pronounced oscillatory component. Thus, their appearance indicates that the irregular component of neuronal activity is synchronized over large cortical distances. In some cases, the CCs show coherency in the oscillatory component of neuronal activity, as is the case in cat visual cortex [15, 16]. The mechanism underlying this synchrony is largely unknown, although in a few cases there is an experimental indication that they are mediated by intracortical interactions [17, 18].

In this paper we explore the hypothesis that chaos generated by the deterministic dynamics of local cortical networks contributes significantly to the observed neuronal stochasticity in cortex, and that the observed neuronal synchrony is due at least in part to the correlations induced by the cooperative dynamics of the local cortical circuits.

These hypotheses raise several fundamental questions. First, are the cellular properties and connectivity patterns of the cortical networks capable of generating strongly chaotic dynamic states? Secondly, are these chaotic fluctuations synchronized across the system? Thirdly, are the patterns of synchronized chaos generated in these networks similar qualitatively to those observed in cortex? And lastly, what are the natural parameters that control the onset of these states and their properties?

In this work we address the above issues in the context of primary visual cortex whose anatomy and physiology have been extensively studied. We model a region of cortex of a linear dimension of the order of 1 mm. This region corresponds roughly to a cortical hypercolumn, namely to a cortical region whose neurons have overlapping receptive fields [19]. The number of neurons in such an area is of the order of $10^5 - 10^6$ neurons, about 80 percent of which are excitatory neurons and the rest inhibitory. Studying the dynamics of a network of such scale can be done only in a dynamical framework appropriate for large systems. An important concept which is central to our work is the *thermodynamic limit*. Specifically, it is assumed that the system architecture and dynamics can be appropriately scaled up to larger sizes so that the behavior will have a well defined limit when the size grows to infinity.

Although this limit is purely theoretical, it is an extremely useful tool in classifying and understanding the behavior of systems with many degrees of freedom.

An example of the use of the thermodynamic limit is the issue of how to characterize the temporal irregularity of the network. In principle, this can be precisely defined using the notion of chaotic attractor in dynamical systems [20]. However, testing whether a large network is in a chaotic attractor, e.g., by measuring its Lyapunov exponents is very difficult. Here we will use the term chaos to mean temporal variation characterized by a broad power spectrum. This will be investigated by the long time behavior of the time-dependent correlation functions. Specifically, we will define the state of the network as chaotic if the correlation functions decay to time-independent limits in time scales that are finite in the thermodynamic limit. Another issue is the characterization of the degree of synchrony. Since all the neurons in the network are communicating at least indirectly, it is clear that their activity will always be correlated to some degree. We will characterize the degree of synchrony using the classification of synchronous and asynchronous states in large networks that was recently introduced, see [21]. Specifically, we will say that a state is synchronous if the magnitude of the CCs between most pairs of neurons remains finite in the thermodynamic limit. In asynchronous states, the CCs are weak in the sense that except for a small number of pairs, most of them decrease to zero as the system sizes grows. States that are both chaotic and synchronous are termed synchronous chaotic (SC) states. The hypothesis of the present work is that the dynamics of cortical networks can be described as SC states.

In order to study the possible generation of SC states by the intrinsic dynamics of the network, we investigate the statistically stationary dynamic properties of a large network governed by *deterministic* dynamic equations with a time-independent external stimulus. In addition, in accord with anatomical and physiological evidence [22], we assume that the number of synaptic connections per neuron is high. The network, however, is not fully connected. The pattern of connectivity has a spatial structure which is correlated with the internal organization of hypercolumns in orientation columns which are labeled by their preferred orientations (POs). Thus, the (excitatory) interactions have a limited range in orientation coordinates. In recent years considerable progress has been made in understanding the cooperative properties of highly connected networks with simplified neuronal dynamics, such as dynamics of two-state neurons or circuit equations of sigmoidal neurons. These simplified models tend to exhibit either fixed points or limit cycles. Temporal fluctuations are incorporated in these models usually by adding external stochastic noise. In order to explore more complex dynamic behavior we incorporate a more realistic model of neuronal dynamics. It is based on a Hodgkin-Huxley type model [23] of an excitable voltage-clamped cell with several cellular and synaptic conductances. The single cell properties of the model are, in general, qualitatively consistent with the available physiological data, although they do not incorporate the full complexity of real neurons in cortex. The complexity of the model precludes analytical study of its properties, hence we use computer simulations to study them.

The present work is an extension of our previous study, reported briefly in [24]. Our earlier model consists of only excitatory neurons and employed instantaneous synaptic inputs. Comparison between the earlier model and the present one will be presented in the Discussion. The temporal variability generated by the deterministic dynamics of neural networks has been investigated by several recent theoretical studies. Bush and Douglas [25] studied the dynamics of a small network of neurons using compartmental models of bursting pyramidal cells with global inhibition. Usher et al.[26] studied networks of integrate-and-fire neurons with two-dimensional architecture and found features resembling self-organized criticality.

1.2. Cortical mechanism of orientation selectivity

The mechanism for the generation of orientation selectivity in the cortex is not fully known [19],[27]-[30]. The input to the cortex is provided by neurons in the lateral geniculate nucleus (LGN), which respond independently of the stimulus orientation. According to the classical model of Hubel and Wiesel, the PO of a cortical cell originates from the geometrical alignment of the circular receptive fields of the LGN neurons that are afferent to it [19]. The experimental evidence of this model is ambiguous. The alignment of the receptive fields of the LGN inputs to a cortical cell apparently parallels the cell's PO [29]. However, suppression of cortical inhibition tends to considerably degrade the orientation tuning [27, 28], suggesting that cortical circuitry plays an important role in shaping the relatively sharp orientation tuning in cortex. Furthermore, estimates based on intracellular measurements indicate that most of the orientation-selective excitatory input to cortical cells comes from cortical feedback [31].

Recently, this issue was studied analytically within a simple neural network model with stochastic, two-state neurons [32]. Using a mean field theory it has been shown that in a suitable parameter regime, the network exhibits orientation selectivity that originates from within the cortex by a mechanism known as spontaneous symmetry breaking [33]. When the input is not oriented, the network has a continuum of states, each representing an inhomogeneous population activity which is peaked at one of the orientation columns. As a result, the network yields a sharp orientation tuning even when the total input from LGN to a cortical neuron is only weakly tuned to the stimulus orientation. This behavior occurs when the cortical interactions decrease strongly with the distance between the columns. When the network exhibits this behavior we will say that it is in a *marginal phase* [34]. Several experimental consequences of this cortical mechanism of orientation tuning have been predicted:
(i) The tuning width is expected to be relatively independent of the contrast and angular anisotropy of the visual stimulus.

(ii) The transient population response to changing of the stimulus orientation is characterized by a transient activation of intermediate orientation columns before the population activity stabilizes around the new stimulus orientation. This response is termed *virtual rotation.*
(iii) Neuronal CCs exhibit long time tails which correspond to slow random fluctuations in the position of the population activity profile. These long time tails depend on the PO of the correlated pair relative to the stimulus. The tails are positive if the stimulus orientation is larger or smaller than both POs. They are negative if the stimulus orientation is at an intermediate angle relative to the neuronal pair. These slow contributions are in addition to a central positive peak resulting from other fluctuating modes which decay quickly.

The above predictions were derived on the basis of a model with a simplified connectivity pattern and, as mentioned above, simplified neuronal dynamics. It was further assumed that the network is in an asynchronous state, so that the temporal fluctuations of the synaptic inputs are negligible. This means that the amplitudes of the CCs are only of the order of $1/N$ where N is the size of the system. In this paper we will use our model of a cortical hypercolumn to study the role of local cortical connections in shaping the orientation tuning. Specifically, we address the question whether the predictions of the above mentioned simplified model are valid also in a network with more realistic dynamics and architecture, which settles into a SC state.

The outline of the paper is as follows. The following Section describes the dynamics and architecture of the model. In Section 3 the simulation results characterizing the variability and synchrony in our model are described. This includes an analysis of the AC and CC functions of the neuronal firing rates. In Section 4 we study the model in a parameter regime where the orientation selectivity is dominated by the cortical interactions. The predictions of the analytical theory of the simplified models are tested. In Section 5 we investigate the dependence of the dynamic properties of the model on the system size, and conclude that the dynamic state found in section 3 is indeed a SC state. We show that in different parameter regimes the network exhibits different cooperative states, such as synchronous oscillatory states and asynchronous states. We also show the desynchronizing effect of external stochastic noise. In Section 6 the results are summarized and discussed. The detailed description of the dynamic equations and the values of the parameters of the models are presented in the Appendix.

2. The model

2.1. Single neurons

The dynamics of single cells is described by a Hodgkin-Huxley type model of an excitable point neuron,

$$C\frac{dV}{dt} = I_{ext} - \sum_i G_i(V)(V - V_i) \quad . \tag{1}$$

The constant C is the cell capacitance and V is its membrane potential. The right hand side incorporates an external current I_{ext} and additional ionic currents described by their conductances G_i and their reversal potentials V_i. In the present work we incorporate the usual sodium (I_{Na}), potassium (I_K), and leak (I_L) currents. The leak conductance is independent of V and determines the passive properties of the cells near resting potential. The sodium and potassium currents are responsible for the spike-generation. Additional currents are a non-inactivating persistent sodium current, (I_{NaP}), and an A- current (I_A). The first current enhances the excitability of the cells at voltages near threshold. This leads to a frequency vs. current relationship that increases continuously from zero, thereby increasing the dynamic range of the neurons. The A-current reduces the gain of the neurons, thereby suppressing their maximal rate [35, 36]. Both currents are known to exist in cortical and hippocampal cells [37, 38, 39]. Parameters of these currents are given in the Appendix. They correspond to a cell with a resting potential: $V_{rest} = -79 \ \ mV$, a threshold potential for spike generation: $V_{thresh} = -68 \ \ mV$, and a membrane time-constant at rest: $\tau_0 = 10 \ \ msec$.

Cortical cells are classified in two classes: excitatory neurons and inhibitory ones. Although the main difference between them is their synaptic interactions, they also differ in their excitability. The response of many pyramidal neurons (which are presumably excitatory neurons) to a step current shows a strong adaptation which seems to be absent in inhibitory neurons [7]. This feature is incorporated in our model by adding an adaptation current to the excitatory neurons. This current is a slow potassium current [40], with a relatively large time-constant (see Appendix).

Examples of the response of excitatory and inhibitory cells to an injection of a current step are shown in Fig. 1. It clearly shows the regular firing of the inhibitory neurons from the onset of the response and the decrease in the frequency of response of the excitatory neurons. Note that neither of the neurons exhibits bursts of action potentials.

In our model, I_{ext} is given by

$$I_{ext} \ = \ I_{syn} \ + \ I_0 \ + \ I_{noise} \tag{2}$$

where I_{syn} denotes the synaptic current generated within the network, and I_0 stands for synaptic currents from sources outside the network. Both of these currents are defined below. In some of our simulations we add an external noise, denoted by I_{noise}

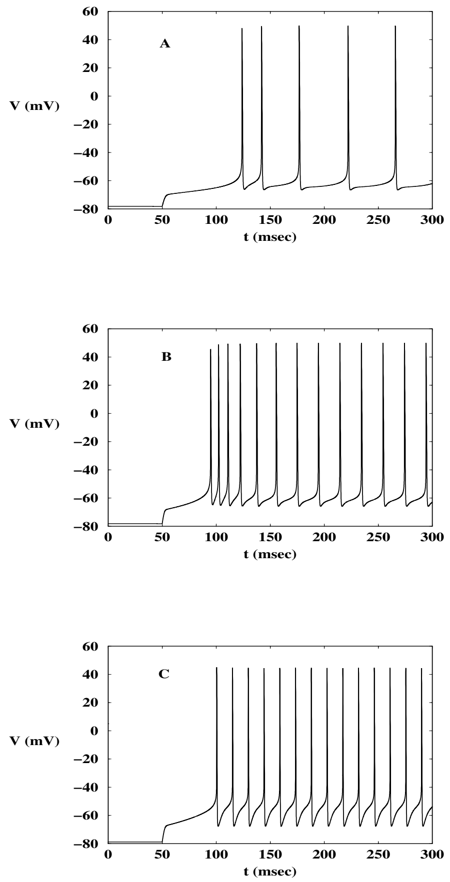

Figure 1: Response of neurons to a depolarizing step of current. The step starts at $t = 50$ $msec$. A: An excitatory neuron with a current $I_{ext} = 3\mu A/cm^2$; B: An excitatory neuron with a current $I_{ext} = 8\mu A/cm^2$; C: An inhibitory neuron with a current $I_{ext} = 5\mu A/cm^2$. The parameters for the dynamics are given in Table I.

(see Appendix for details on the form of I_{noise}).

2.2. Synaptic interactions

Synaptic inputs are modeled as conductance changes. The synaptic current flow into a cell at time t, induced by a single presynaptic spike at time t_0 is

$$I_{syn}(t) = G_{syn} f(t - t_0)(V_{syn} - V(t)) \tag{3}$$

An action potential is said to occur at time t if the membrane potential (of the presynaptic cell) crosses at that time a threshold value, taken here as $-20\ mV$, with a positive slope. The constant G_{syn} represents the peak value of the synaptic conductance. Its time-course is described by $f(t)$,

$$f(t) = A\left(e^{-t/\tau_1} - e^{-t/\tau_2}\right) \tag{4}$$

for $t \geq 0$ (and $f(t) = 0$ otherwise). The normalization constant A is such that the peak value of f is 1. The characteristic times τ_1 and τ_2 are respectively the synaptic rise time and decay time. In our model, both time constants are in the range of $1 - 10\ msec$. We do not consider here the effects of slow synapses, such as inhibition mediated by $GABA_B$ and excitation that is mediated by $NMDA$ transmitters. For multiple events, $I_{syn}(t)$ becomes the sum of the total contributions at time t of all spikes generated by the presynaptic cells in the past.

2.3. Network architecture and inputs

The network models a hypercolumn of visual cortex. It consists of N_E excitatory neurons (denoted by E) and N_I inhibitory neurons (denoted by I) that respond to an oriented visual stimulus in a common receptive field. The ratio between the size of the two populations is $N_I/N_E = 0.2$. The total size of the network is denoted by N, $N = N_E + N_I$. Excitatory neurons in the hypercolumn are characterized by an angle which denotes their PO. A neuron with a PO θ responds maximally to a stimulus with an orientation angle θ. This PO is at least partially due to the geometric alignment of the receptive fields of the input to the cells from the early stages of the visual pathway, namely from the LGN [19]. These anisotropic inputs are modeled as external currents, which contribute to the RHS of Eq. (1). The input to a cell with a PO θ due to a visual stimulus with an orientation θ_0, is given by

$$I_0 = F(|\theta - \theta_0|) \tag{5}$$

where $F(\theta)$ is a monotonic decreasing function of $|\theta|$, with a peak at zero. Note that since we focus primarily on the steady state properties of the network these inputs will be assumed, in most of the work, to be time-independent. The form of $F(\theta)$, chosen for the inputs to the excitatory neurons is shown in Fig. 2A.

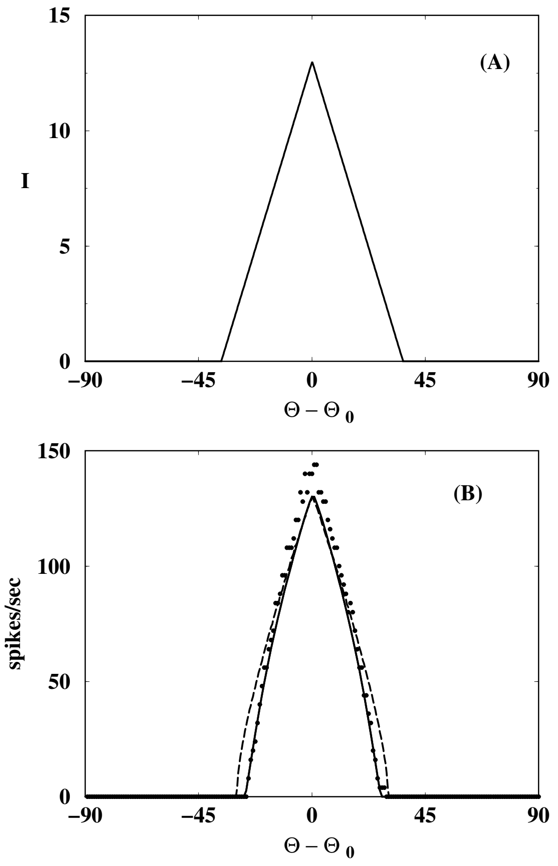

Figure 2: A: The input to an excitatory cell of PO θ due to a visual stimulus with an orientation θ_0. The abscissa is in degrees; The ordinate is the input current in $\mu A/cm^2$. B: Dashed lines:The orientation tuning curve Γ of a single isolated excitatory neuron with PO θ upon stimulation of a bar with orientation θ_0 vs. $\theta - \theta_0$ in degrees. Full line: The tuning curve of a neuron in the SC state. The activity of the neuron is averaged over 18 sec after stimulus onset. The dots correspond to the activity averaged over 200 $msec$ after after stimulus onset.

This curve represents the orientation tuning of the LGN input to cortical cells. Figure 2B displays the orientation tuning of the excitatory neurons in the absence of inputs from the network. This tuning is represented by the function $\Gamma(\theta - \theta_0)$ which measures the average frequency of firing of an isolated excitatory neuron θ responding to a stimulus θ_0.

For practical reasons we assume that inhibitory neurons do not display a response which is selective to the stimulus orientation. The external currents received by the inhibitory neurons are randomly distributed with a homogeneous distribution that ranges between $I_{min} = 0\mu A/cm^2$ and $I_{max} = 5\mu A/cm^2$.

We assume the following pattern of synaptic connections in the network. The connectivity inside the excitatory population is high but limited in its range and depends on the difference between the POs of the presynaptic and postsynaptic neurons. Excitatory connections exist and have a peak conductance G_{EE} only if the POs of the pre-and postsynaptic neurons differ by an amount which is smaller in absolute value than a given value $\Delta\theta_0$. If the difference is larger than $\Delta\theta_0$ the two neurons are not interacting. In the model we will choose: $\Delta\theta_0 = 22.5^o$. The inhibition is assumed to be global. Every inhibitory neuron is making inhibitory synapses on all the other inhibitory neurons with a peak conductance G_{II} which is the same for all the inhibitory neurons. Similarly, each inhibitory neuron inhibits all the excitatory neurons with a synaptic strength G_{EI}. The synaptic action of the excitatory neurons on the inhibitory neurons is also assumed to be global with a peak excitatory conductance G_{IE}. The architecture of the network is sketched in Fig. 3.

3. Results

The network dynamic equations have been studied by numerical simulations, using a 4-th order Runge-Kutta method. In most of our simulations the time step was $dt = 0.05 \ \ msec$. Stability and accuracy of the results were checked with time step $dt = 0.025 \ \ msec$. In this Section we describe the behavior of the network in a parameter regime where it exhibits temporally irregular behavior with a significant degree of synchrony. In Section 5 we will analyze the size dependence of the network behavior and will show that in this parameter range the network state should be classified as a SC state. Here we will present results for the parameter values that are listed in Table 2 of the Appendix (Column denoted SC). The orientation of the stimulus is assumed to be $\theta_0 = 0^o$. The results were obtained by averaging over long time (up to 524 sec) for a network size $N_E = 200$ and $N_I = 40$. The initial conditions of the network correspond to spontaneous firing at a rate of about 1 Hz.

3.1. Single neuron responses

In Fig. 2B we plot the average response of a single neuron vs. the difference

Figure 3: Sketch of the architecture of the hypercolumn. The notations are defined in the text.

between its preferred orientation and the orientation of the stimulus. Because of the underlying symmetry of the model network this orientation tuning curve also represents the time-averaged population activity profile defined as the function $\Gamma(\theta - \theta_0)$ where $\Gamma(\theta) = N_{sp}(T,\theta)/T$, $N_{sp}(T,\theta)$ being the total number of spikes emitted during a sufficiently long time T by a neuron with PO θ.

The curve displayed in Fig. 2B corresponds to an averaging over the first $18sec$ after the onset of the stimulus. The profile has a width $\approx 60^o$, corresponding to the activation of about 1/3 of the neurons of the network. The other neurons do not fire at all because they do not receive a sufficient total input from the stimulus and from the network. The spread in the firing rates is large, with a maximum rate of 130 $spikes/sec$. A very similar tuning curve is obtained by averaging over a shorter time interval as shown in Fig. 2B, indicating that the network settles into its stationary regime within a hundred milliseconds.

The traces of the membrane potentials of six neurons with different POs are shown in Fig. 4. The substantial temporal irregularity seen in this figure arises from the network dynamics, as we have not introduced any stochastic noise into the system.

The traces show that neurons with POs closer to the orientation of the stimulus have a strong tendency to burst, with substantial variations in the number of spikes within the bursts as well as in the interburst time intervals. Within a burst, the interspike intervals decrease in time, a fact which results from the presence of the adaptation current. In contrast the spikes of neurons with lower firing frequency are frequently isolated.

A quantitative measure of the temporal variability of the activity of a neuron is obtained by calculating the auto-correlation (AC) function of its spike train. The AC of a spike train of a neuron i, $C_{ii}(\tau)$, is defined as the time-delayed AC of the instantaneous rate $S_i(t)$. The variable $S_i(t)$ is $1/\delta$ if the neuron emits a spike within a time bin of δ about time t and zero otherwise. Thus,

$$C_{ii}(\tau) = \langle S_i(t) S_i(t+\tau) \rangle \tag{6}$$

where $\langle ... \rangle$ means average over t, using a long time window. Note that with this definition the AC's are measured in $(spikes/sec)^2$ (if time is measured in seconds). Figure 5 presents the ACs of the spike trains ($\delta = 0.25$ $msec$) of the six excitatory neurons shown in Fig. 4. They were computed over a run of 524 sec and the results have been smoothed by Gaussian filter with a variance of 0.5 $msec$.

The ACs display a deep trough near $\tau = 0$, which corresponds to the refractoriness of the neurons. In addition, several relatively sharp peaks occur within the central deep 'valley'. These indicate a relative increase in probability of firing within short times after a given spike, which reflects the tendency of the neurons to fire bursts of spikes. Many of the ACs display additional peaks at $60 - 100$ $msec$. As can be seen in the figure, these damped oscillations are pronounced in neurons with low firing rate.

Another measure of the statistics of spike trains is their interspike histograms. The interspike histograms of the above 6 neurons is depicted in Fig.6. It shows

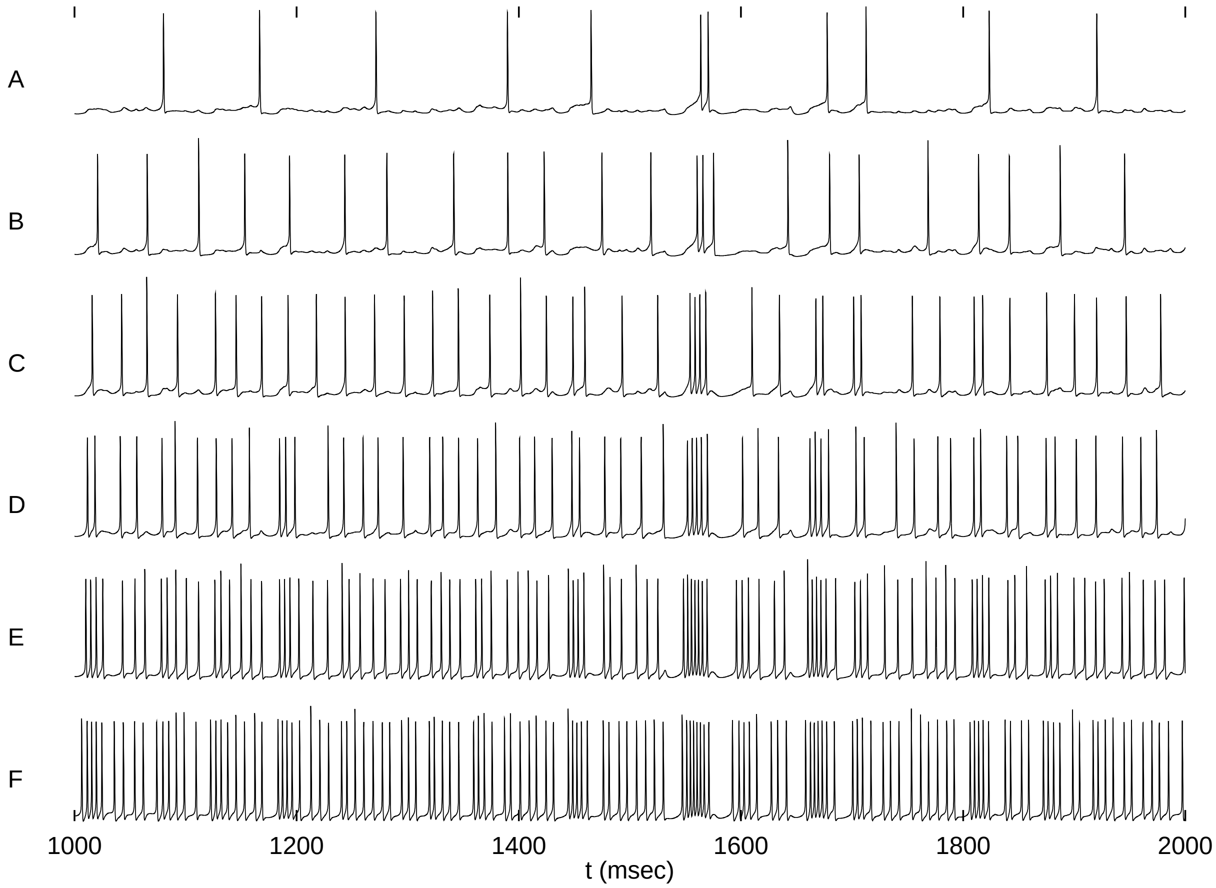

Figure 4: Membrane potential of six excitatory neurons in the SC state. The orientation of the stimulus is $\theta_0 = 0$. The POs of the neurons are from bottom to top: 0^o, 8.1^o, 17.1^o, 20.7^o, 23.4^o, 25.2^o.

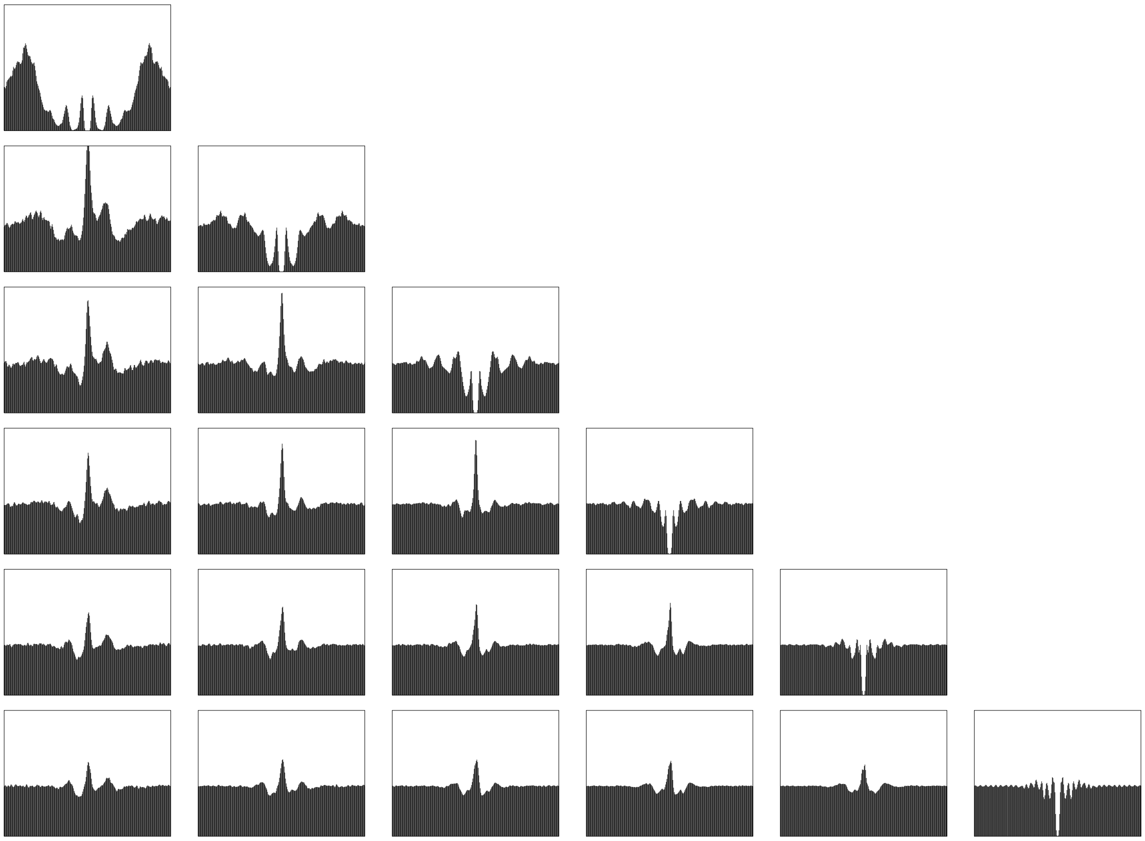

Figure 5: Autocorrelograms (diagonal) and crosscorrelograms (off-diagonal) of the six neurons shown in Fig. 4 for time delays between -125 $msec$ and 125 $msec$. The AC are normalized to the square of the firing rates of the neurons and the CCs to the product of the firing rates of the two neurons of the pair. The ACs and CCs therefore reach 1 at large time delays. The ACs and CCs were calculated from spike trains with total length 524 sec with bins of 0.25 $msec$ and were smoothed with a Gaussian filter of variance 0.5 $msec$.

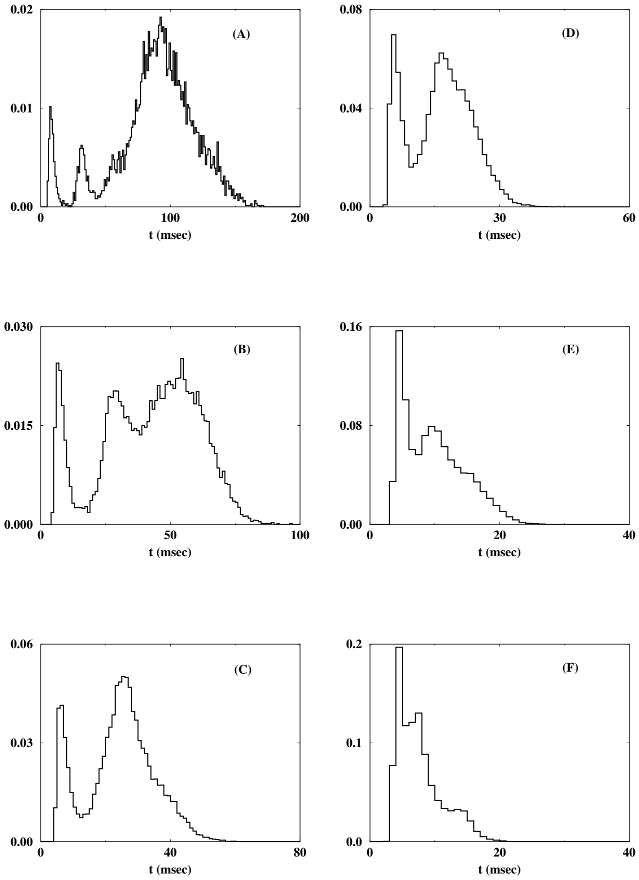

Figure 6: Interspikes interval histograms (bin of 1 $msec$) of the 6 neurons shown in Fig. 4.

a multimodal structure, particularly pronounced in the low firing neurons. This structure indicates the tendency of the neurons to fire in bursts.

3.2. Synchrony

The traces of Fig. 4 show that a large proportion of the spikes of the different neurons are synchronized. This synchronization is reached already after $300-500$ $msec$ of activation of the network. The fact that the network is strongly synchronized can also be seen from the strong temporal fluctuations of the membrane potential averaged over the entire excitatory population whose AC is shown in Fig. 7.

A quantitative measure of the synchrony between a pair of neurons is provided by the cross-correlations (CCs) of spike trains of pairs of neurons. Similar to the AC, Eq. (6) the CC, $C_{ij}(\tau)$, of spike trains of neurons i and j is defined as an average

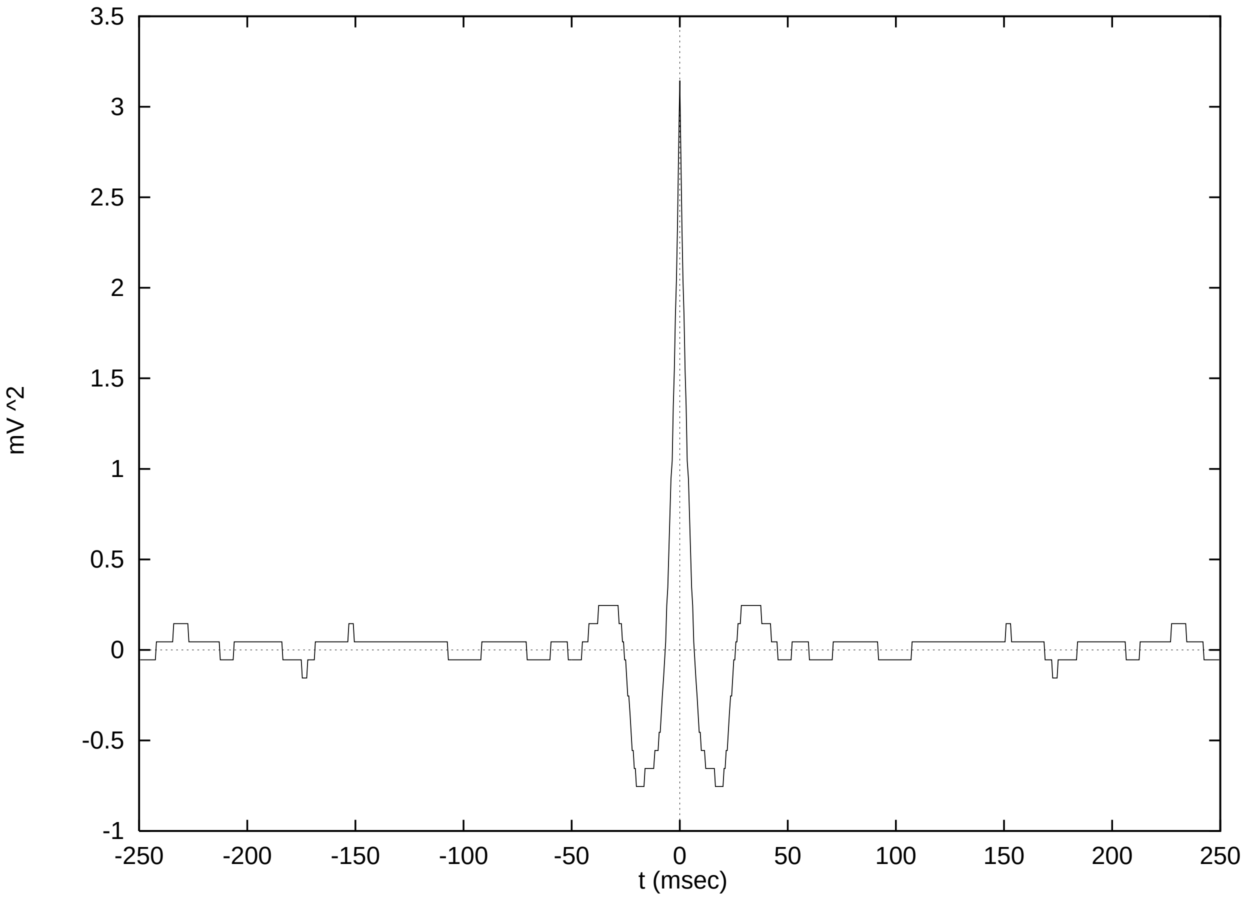

Figure 7: The AC of the membrane potential averaged over the entire excitatory population ($\bar{V}(t) = \frac{1}{N_E}\sum_{i=1}^{N_E} V_i(t)$) in the SC state. The substracted AC ($\langle \bar{V}(t)\bar{V}(t+\tau)\rangle - \langle \bar{V}(t)\rangle^2$) is plotted. Network with $N_E = 400, N_I = 80$.

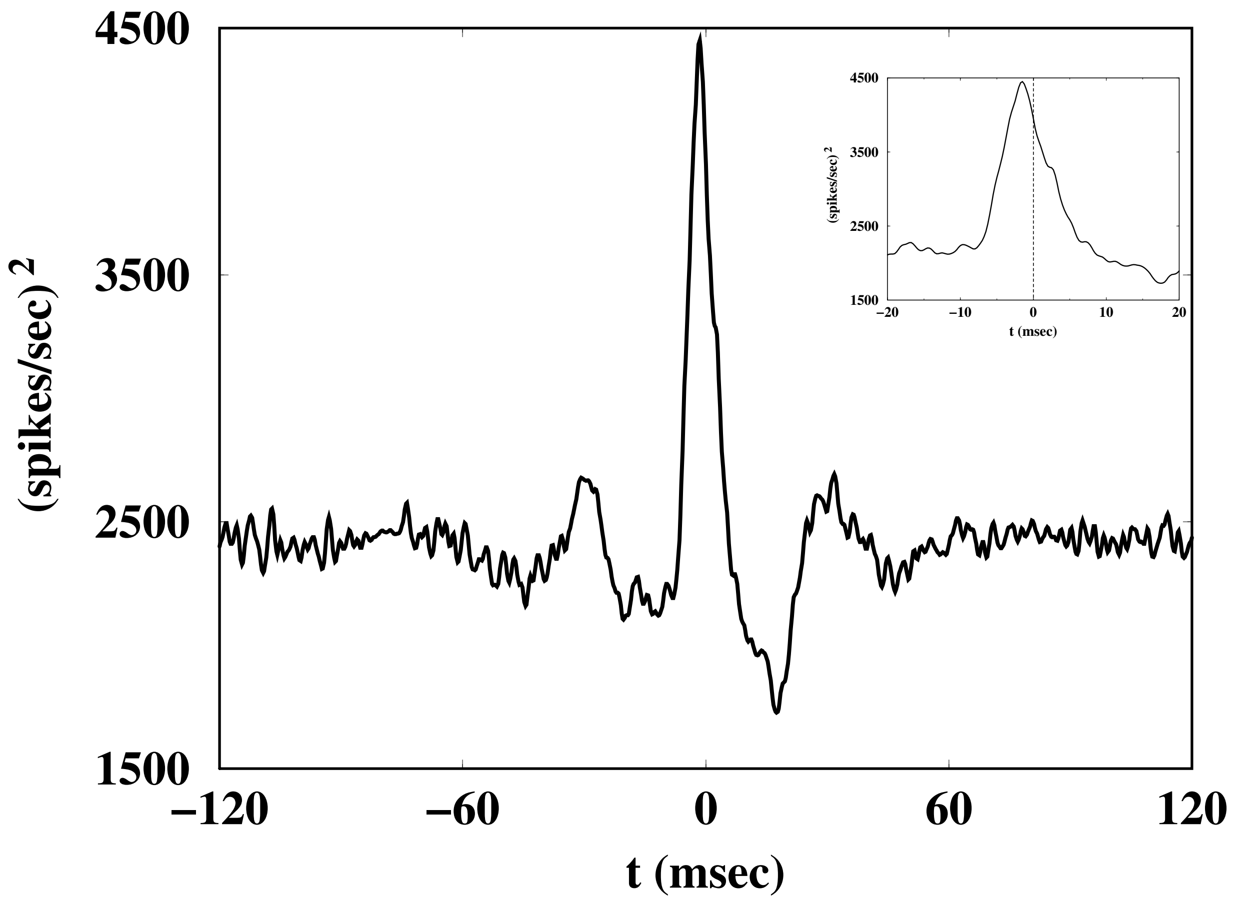

Figure 8: The CC between a neuron with PO $\theta = 9^o$ and a neuron with PO $\theta = 24.3^o$. The negative time shift of the peak means that the second neuron tends to fire after the first one. Inset: The central region of the CC.

over t of the product of $S_i(t)$ and $S_j(t + \tau)$,

$$C_{ij}(\tau) = \langle S_i(t) S_j(t + \tau) \rangle \quad . \tag{7}$$

The CCs of several pairs of excitatory neurons are plotted in the off-diagonal part of Fig. 5. A common feature of the CCs is the fact that they are nonoscillatory. In general, they display a strong central peak accompanied by troughs and possibly secondary peaks.

An interesting feature is the shift of the maximum of the CC from $\tau = 0$, in most of the CCs. An example is shown in Fig. 8. These shifts are of the order of $1 - 3$ $msec$ and are correlated with the difference in the firing rates of the two neurons in the pair. Their signs are such that the neuron with higher firing rates leads over the one with lower rate. The magnitude of the shift is relatively large for pairs of neurons with very different rates, and they disappear for neuronal pairs with the same POs.

4. Cortical mechanism of orientation selectivity

In the parameter regime studied above, the orientation tuning was produced by assuming that the input from the LGN, i.e., I_0, Eq. (5), is strongly tuned to the stimulus orientation, see Fig. 2. In fact, with the above parameters the tuning of the activity of an isolated neuron is only mildly broader than that of the neuron in the network (compare the dashed line and the full line in Fig. 2B).

As mentioned in the Introduction, it was predicted in an earlier work [32] that if the orientation dependent component of the cortical interactions is strong enough compared to the inverse gain of single neurons, then the system will exhibit a marginal phase where even in the absence of orientation specific input the system will spontaneously form a spatially inhomogeneous activity profile. In this *marginal phase* the orientation tuning of the system, in the presence of weakly tuned stimulus, is strongly enhanced by the cortical feedback interactions. In this Section we address the following questions: Is there a range of parameters for which our model shows a similar enhancement of orientation tuning by the 'cortical' feedback interactions? If yes, what are the dynamical properties of the network in this parameter range? We have found that for a sufficiently low value of g_z, a marginal phase appears. This will be shown below for network parameters that are the same as for the previously described SC state except that $g_{EI} = 4\ mS/cm^2$, and $g_z = 0$. We will also show that in this set of parameters the system exhibits synchronized, temporal variability characteristic of a SC state.

4.1. Tuning curve properties

To establish the existence of the marginal phase we first examine the case of isotropic external input.

Figure 9A shows the population activity profile of a network with an input on the excitatory population which is $I_0 = 4\ \mu A/cm^2$ for all θ (the input on the inhibitory neurons is the same as in section 3) . The position of the population activity profile is determined purely by the inhomogeneity induced by the initial conditions which were used to initialize the network, which is the characteristic of a marginal phase. Figure 9B shows the tuning curve in the presence of a weakly tuned input peaked at $\theta_0 = 0^o$ (dotted line in Fig. 9B). We measure the magnitude of the input tuning by $\epsilon \equiv (I_{max} - I_{min})/(I_{max} + I_{min})$. Here $\epsilon = 0.025$. By comparing with Fig.9A, it can be seen that the system of Fig. 9A acts as if there is an external stimulus at an orientation 30^o. The tuning width of the two figures is the same, indicating that it is determined by the cortical interactions. The weakly tuned stimulus fixes the position of the activity profile. It selects among the set of attractors the one that

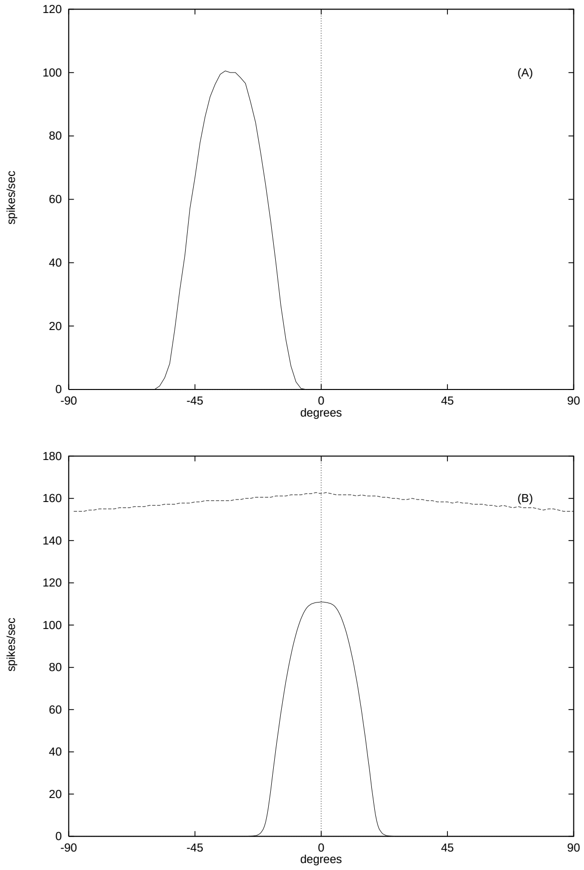

Figure 9: A: Population activity profile for $\epsilon = 0$. B: Tuning curve in the presence of weak input tuning $\epsilon = 0.025$. The dotted line corresponds to the tuning curve of the isolated neuron.

best matches its own profile, namely the one that peaks at the orientation column that has the largest input.

4.2. Virtual rotation

Previous work [32] has shown that the transient response of the system to a step change in the orientation of a stimulus is an indicator of the mechanism of orientation selectivity. If the alignment of the afferent LGN input is the main mechanism, then following a change in the stimulus orientation, the activity in previously stimulated columns will decay, while the activity of the columns with POs close to the new stimulus orientation will increase. On the other hand, if the spatial modulation of the cortical interactions plays a dominant role, then the population activity will move across the cortex, activating transiently the intermediate column until it settles in the new stable position. This response was termed *virtual rotation*.

To test whether this prediction holds also in our more realistic model, we have calculated the response of the system to changing of the stimulus orientation. Figure 10A shows the evolution in time of the activity profile following a change of 60^o in the stimulus orientation. The anisotropy is $\epsilon = 0.2$. It shows clearly the phenomenon of virtual rotation. For comparison we show in Fig. 10B the corresponding results for the parameter regime of the previous Sections. It should be emphasized that there is a considerable difference in the response times in the two cases. In the case of strong input tuning (Fig. 10B), the profile settles in the new position rapidly, within 50 $msec$, whereas the virtual rotation (Fig. 10A) is considerably slower, settling around the new orientation column only after several hundred $msec$.

Further demonstration of the successive activation of intermediate columns is given in Fig.11, which shows the time course of the membrane potentials of four neurons. Neurons D and C, with POs 0^o and 10^o, respectively, are "turned on" following the onset of the first stimulus at time 250 $msec$. The membrane potential of neuron B with $\theta = 30^o$ is increased at the onset of the stimulus but no action potential is produced due to inhibition and the membrane potential decays again. Neuron A, with $\theta = 60^o$, is inactive. When the stimulus changes orientation to 60^o at 750 $msec$, the activity of neuron D decays within 100 $msec$ whereas neuron C increases its activity and remains active until 900 $msec$. Neuron B is activated at 850 $msec$ and remains active until 1100 $msec$. Finally, neuron A is turned on at 950 $msec$ and remains highly active for the duration of the stimulus.

4.3. Correlation functions in the marginal phase

The mean field theory predicted that in the marginal phase broad CCs will appear due to slow random collective fluctuations in the position of the population activity profile. These long time tails of the CCs depend on the PO of the correlated pair

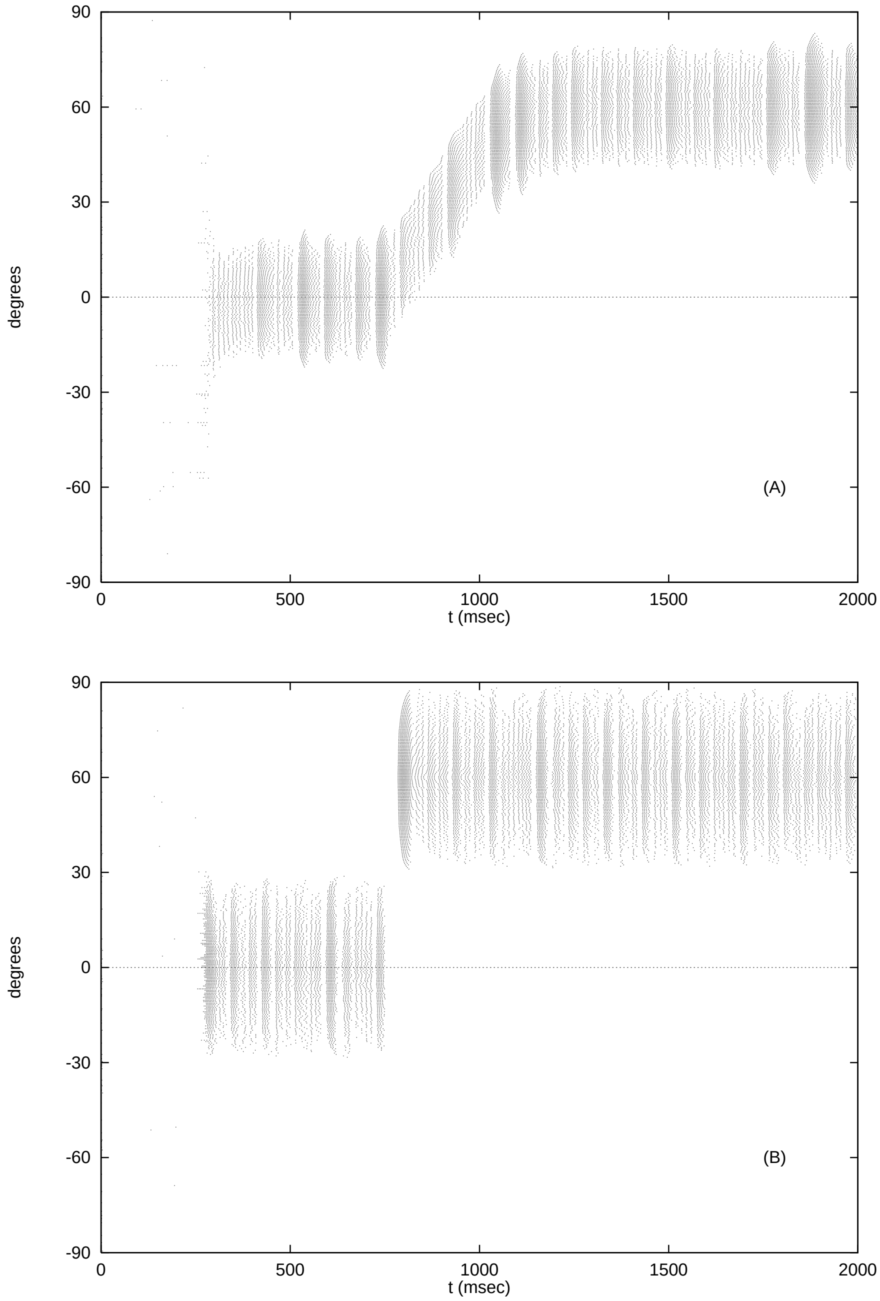

Figure 10: Raster plots of the activity of the network. A stimulation at $\theta_0 = 0^o$occurs after a period of 250 $msec$ of spontaneous activity. The stimulus is rotated to $\theta_0 = 0^o$ at $t = 750$ $msec$. A: The parameters of the network are those of Section 4 (the orientation tuning dominated by the cortical mechanism). The input tuning is $\epsilon = 0.2$. B: The network is in the regime of Section 3.

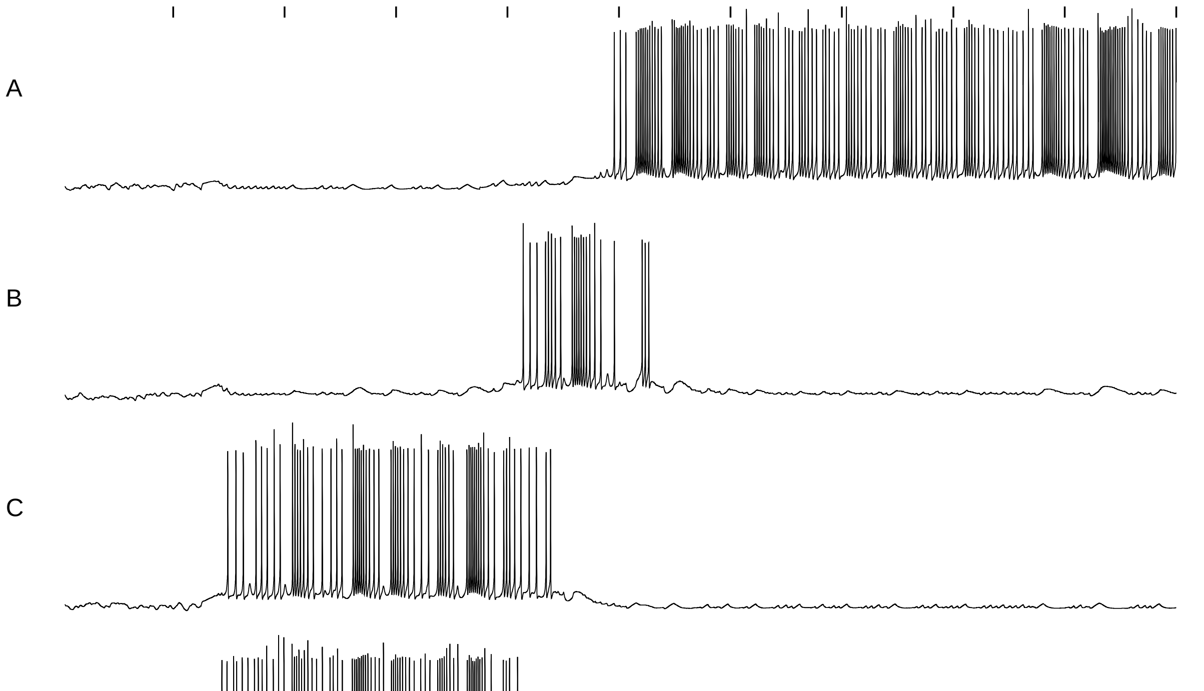

Figure 11: The membrane potential of 4 neurons during stimulation and rotation of stimulus by 60^o. The POs of the plotted neurons are: A: $\theta = 60^o$; B: $\theta = 30^o$; C: $\theta = 10^o$; D: $\theta = 0^o$

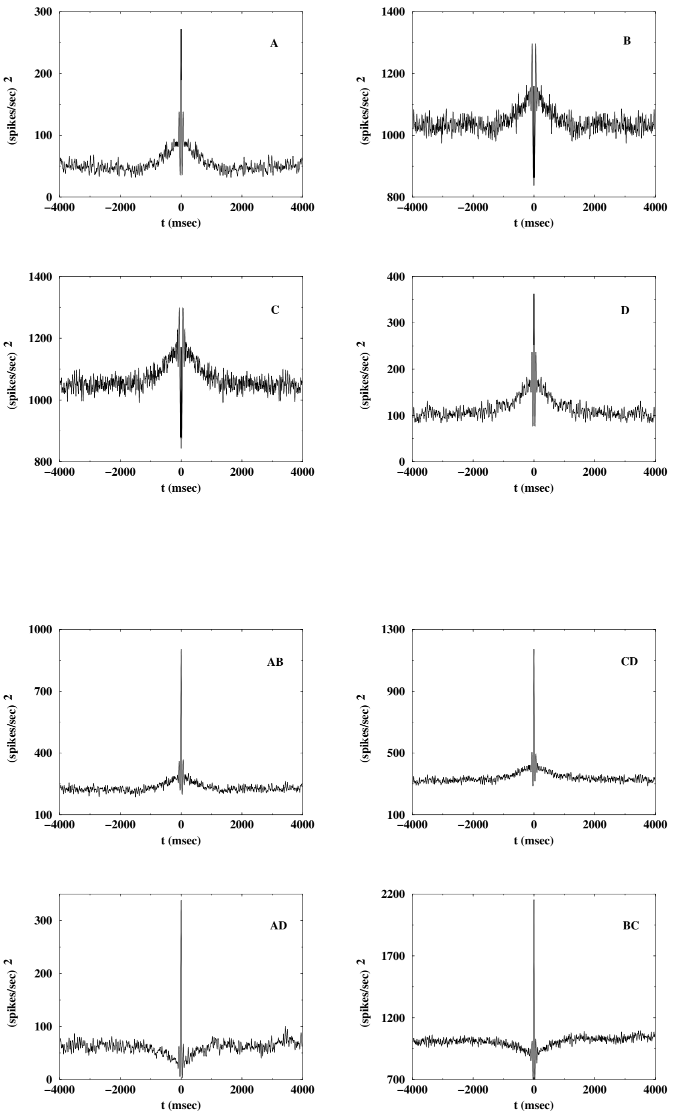

Figure 12: AC and CC of the spike trains of 4 neurons. The length of the spike trains was 140 sec and the results were smoothed with a gaussian filter of variance 9 $msec$. $A : \theta = -19.4^o$, $B : \theta = -17.1^o$, $C : \theta = 17.1^o$, $D : \theta = 19.4^o$. Stimulus at 0^o.

relative to the stimulus. The tails are positive if the stimulus orientation is larger or smaller than both POs. They are negative if the stimulus orientation is at intermediate angle relative to the neuronal pair. These slow contributions are in addition to a central positive peak which results from other fluctuating modes which decay quickly.

As mentioned already, the above predictions were based on calculations of the CCs in a network which is in an asynchronous state due to strong stochastic noise. Here we check the above predictions in the context of our deterministic model with synchronized chaos.

Figure 12 shows ACs and CCs among four neurons. All ACs show a narrow central peak riding on top of a broad 'hill'. The existence of two time scales are also seen in the CCs. However the sign of the slow component depends on the position of the pair relative to the stimulus orientation. Pairs AB and CD are at the same side of the population activity profile. They exhibit long positive time tails as predicted.

AD and BC are examples of pairs that are at opposite sides of the tuning curve. Their correlations possess negative long time tails. It should be stressed that the long time tails in the correlation functions are very sensitive to the magnitude of the input anisotropy. In fact, in order to observe them in the present simulations in a reasonable time averaging we used the value $\epsilon = 0.025$.

5. Nature of the Chaotic State

5.1. Thermodynamic limit

The dynamic behavior of a network may be sensitive to the precise details of the parameters that characterize its dynamics and connections. It is thus very important to understand the generality of the behavior observed in the simulations. One of the parameters is the size of the network, N. Studying the size dependence of the results is extremely important for several reasons. First, systematic numerical simulations of networks such as ours with reliable statistics are limited to sizes of up to several hundred neurons. This limitation is more severe for more complex networks, e.g., networks with spatially extended cells. Although the relevant scale of local circuits in cortex is not known, it is quite possible that it involves at least several thousands of neurons. More importantly, understanding the size dependence is crucial for understanding the qualitative nature of the dynamic state in networks with high connectivity. This is because in such networks there is usually a large separation in scale between the magnitude of the individual synaptic inputs and the total synaptic inputs to a cell. Finally, the size-dependence can give an important clue on the robustness of the results to various perturbations, as will be shown below.

In order to discuss the size-dependence of the dynamic behavior of the network we have to specify how the network parameters vary when N is increased. Here we assume that the single cell properties, including its time-constants, the resting and threshold potentials, as well as the external current, I_0, are independent of N. This implies that the total synaptic input I_{syn} must remain of order unity as N grows. Excluding precise cancellations, the size of the amplitude of most of the individual synaptic inputs must be inversely proportional to N. In our case it means that

$$G_{EE} = \frac{g_{EE}}{N_E} \ ; \ G_{IE} = \frac{g_{IE}}{N_E} G_{EI} = \frac{g_{EI}}{N_I} \ ; \ G_{II} = \frac{g_{II}}{N_I} \tag{8}$$

where the normalized conductances, g_{EE}, g_{IE}, g_{EI}, and g_{II} are independent of N_E and N_I.

5.2. Classification of degree of synchrony

Given the above scaling of the synaptic conductances, there are several ways in which the system size can affect the dynamics of the network. However, as discussed in Ref. [21] there are two simple generic cases. These cases are termed *asynchronous* and *synchronous* states, and they differ in the way the temporal fluctuations of the total synaptic conductance change with N.

In asynchronous states the total synaptic excitatory and inhibitory conductances of a neuron generated by the network approach a time-independent limit as $N \to \infty$. This reflects the fact that the action potentials of the of individual neurons are very weakly synchronized. Summing N temporally uncorrelated (or weakly correlated) contributions results in a total synaptic conductance whose fluctuations has an amplitude of order $1/\sqrt{N}$. Such a state can be self-consistent because the weak temporal variation in the "common input" to the different neurons may be insufficient to synchronize them. Characterizing this state can be done in two ways. One is by evaluating a global variable, e.g., the spatially averaged instantaneous activity. In the asynchronous state the variance of such a quantity vanishes as N increases, typically as $1/N$. Alternatively, one evaluates the CCs between pairs of neurons. The magnitude of the typical CCs will be of the order of $1/N$.

In synchronous states there are temporal fluctuations on a global scale. The variance of the global activity, as well as the variance of the total synaptic conductance of a neuron, remain of order unity even for large N. This implies, of course, that the degree of synchrony generated by the common input from the rest of the network is itself of order unity even in the limit of large N.

The above criterion of synchrony is difficult to check directly in experimental systems since it requires reliable estimates of parameters such as the size of the network and the strength of connections. An alternative criterion is based on the behavior of population averages. Let us denote by $x_i(t)$ a local observable, e.g., the instantaneous rate of the i-th neuron. Let us suppose that we can measure the means of this quantity over a subpopulation of size K, where $K << N$, yielding

$$X_K(t) \equiv \frac{1}{K} \sum_i^K x_i(t) \tag{9}$$

Asynchronous states can be distinguished from synchronous states according to the K dependence of the variance of X,

$$\Delta(K) \equiv \langle (X_K(t) - \langle X_K \rangle)^2 \rangle \tag{10}$$

where $\langle ... \rangle$ denotes averaging over time. In an asynchronous state the local variables are weakly correlated hence

$$\Delta(K) \propto \frac{1}{K} \quad , 1 \ll K \ll N \tag{11}$$

On the other hand, in synchronous states

$$\Delta(K) = O(1) \tag{12}$$

even for large K. The advantage of this criterion is that it does not rely on the absolute scale of Δ, but on its dependence on K which, unlike N, can be varied experimentally. The limitation of this criterion is that the sampling of the x_i's and the value of K should be such that the sums are not dominated by unusually strongly correlated variables. Also, the choice of the variable x_i must be done with care in cases where destructive interference between different types of neurons, which fluctuate out of phase from each other, is likely to occur.

5.3. Synchronous and asynchronous states in the model network

SC state: In order to check whether the chaotic state described in the two previous Sections is indeed a synchronous state, we have simulated networks with different sizes, changing the synaptic conductances according to the scaling of Eq. (8). The ratio between the number of excitatory and inhibitory neurons as well as the other parameters remained unchanged. Here we will present the results for the parameters of Section 3. We have established that qualitatively similar results hold for the parameters of Section 4.

Figure 13 compares the AC of the mean instantaneous firing-rate of the excitatory population, $S(t)$, for $N_E = 200 - 1600$. This rate is defined as the instantaneous rates $S_i(t)$ averaged over all the excitatory population. It is clearly seen that the magnitude as well as the shape of the AC do not change significantly with N, indicating that the temporal variations of the mean activity, which reflect the synchrony in the system, remain the same in the limit of large N.

The effect of changing N on the local fluctuations is shown in Fig. 14, where the AC of the activity of the maximally stimulated neuron is shown for $N_E = 200$ and 800. The overall magnitude and shape of the AC are similar, although some differences are seen. These differences could originate from residual N dependence or from insufficient time averaging.

We have also measured the fluctuations of the instantaneous rate of subpopulations, $S_K(t)$. This quantity is defined as the average of $S_i(t)$ over a subpopulation of K excitatory neurons. It thus corresponds to Eq. (9) with $x_i(t)$ being the instantaneous rate $S_i(t)$. Figure 15 displays the variance of S_K vs K. It clearly approaches a nonzero value for large K confirming the prediction of Eq. (12) for synchronous states.

Synchronous oscillatory states: To obtain insight about the possible effects of the system size we compare the above behavior to a system which is in a synchronous oscillatory state. Such a state is observed in our network in a wide range of parameters. As an example we consider the case of a network with fast excitatory synapses and a relatively weak inhibition. The parameters are given in Table 2 of the Appendix. For small N, we observe a substantial degree of temporal noise.

This is demonstrated in Fig. 17A which shows a non-oscillatory AC of the activity

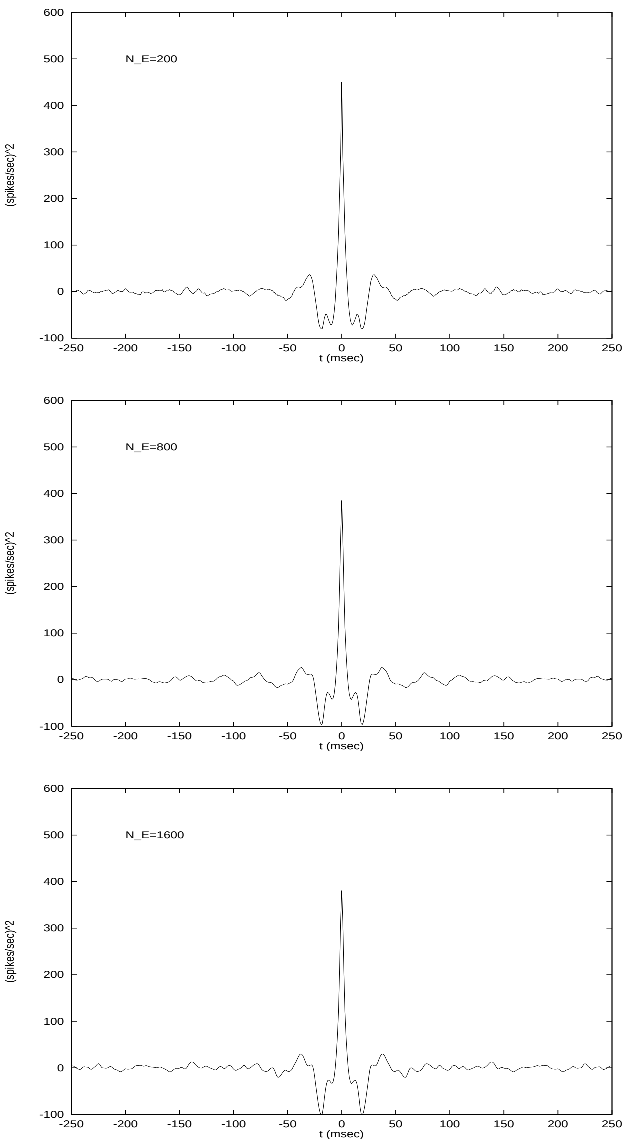

Figure 13: The AC of the mean instantaneous firing rate ($\delta = 1 \quad msec$) of the excitatory population (see the definition in the text) in the SC state for different sizes of the network.

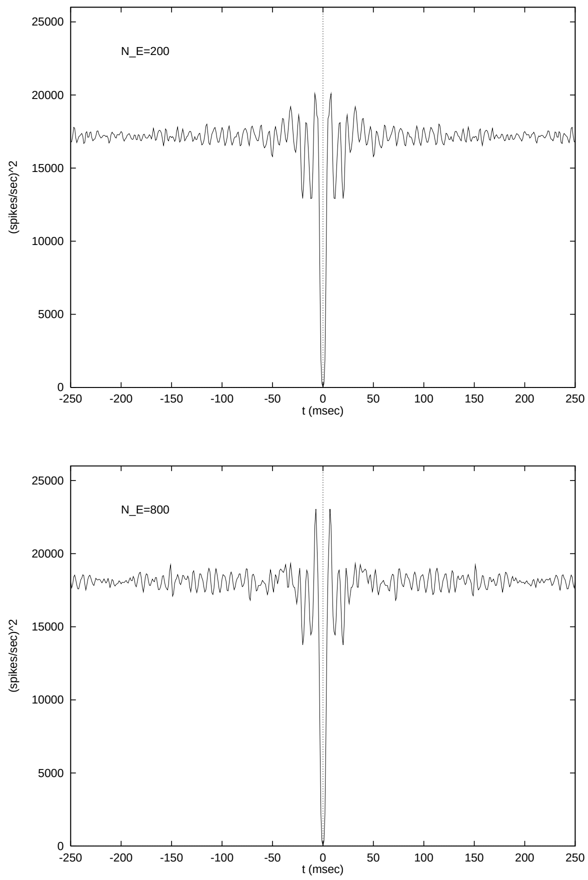

Figure 14: The AC of the activity of the maximally stimulated excitatory neuron for $N_E = 200, N_I = 40$ and $N_E = 800, N_I = 160$. The AC has been smoothed with a Gaussian filter of variance 1 $msec$.

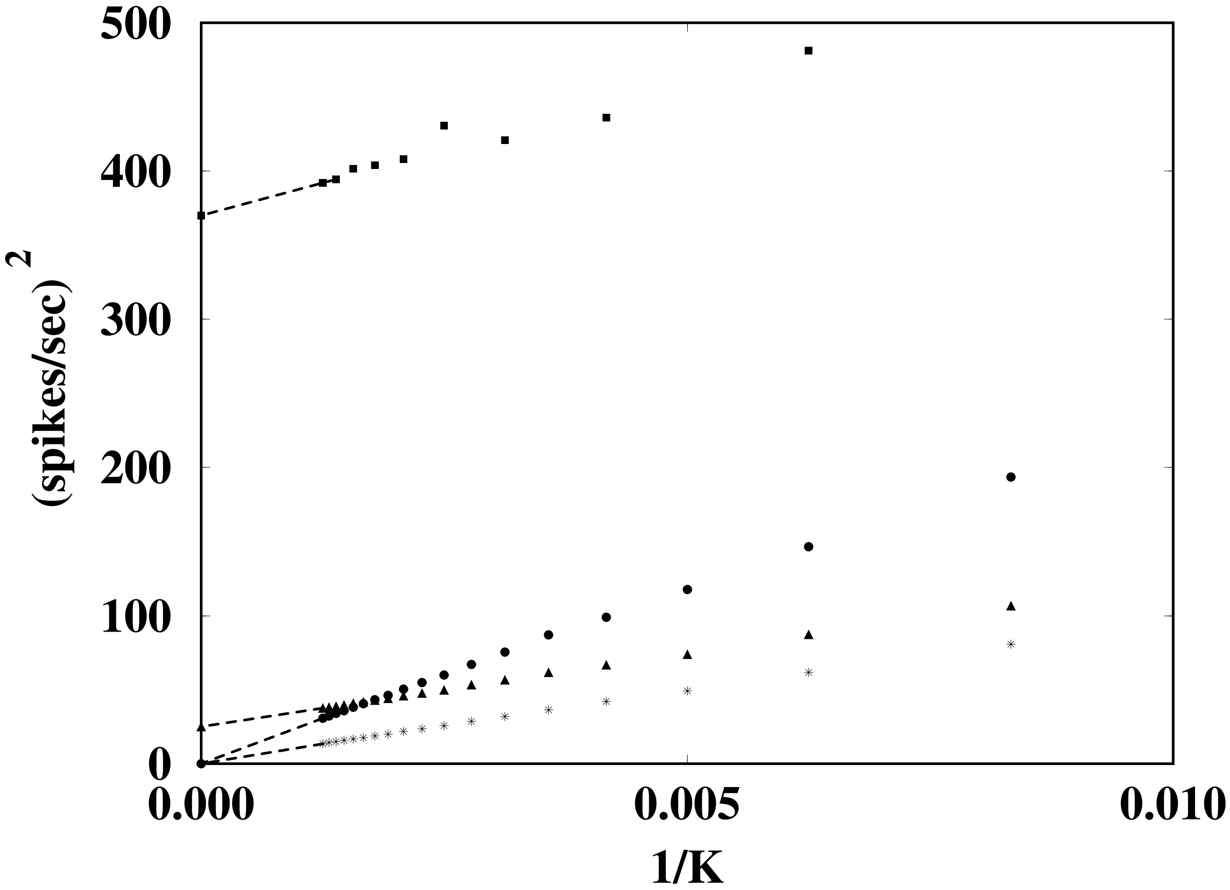

Figure 15: Variance of $S_K(\delta = 1 \;\; msec)$ versus $1/K$ in a network with $N_E = 800$ and $N_I = 160$. For each K, 100 realizations of the subpopulation were chosen at random. For each realization the mean activity of the subpopulation was computed over a time interval of 18 sec and its variance was evaluated according to Eq. (9). Finally, the variance was averaged over the 100 realizations. Dots: Asynchronous state (free of noise). Squares: SC state. Stars: large noise amplitude ($\sigma = 4 \;\mu A/cm^2(msec)^{1/2}$); other parameters are those of the SC state. Triangles: small noise amplitude ($\sigma = 2 \;\mu A/cm^2(msec)^{1/2}$); other parameters are those of the SC state.

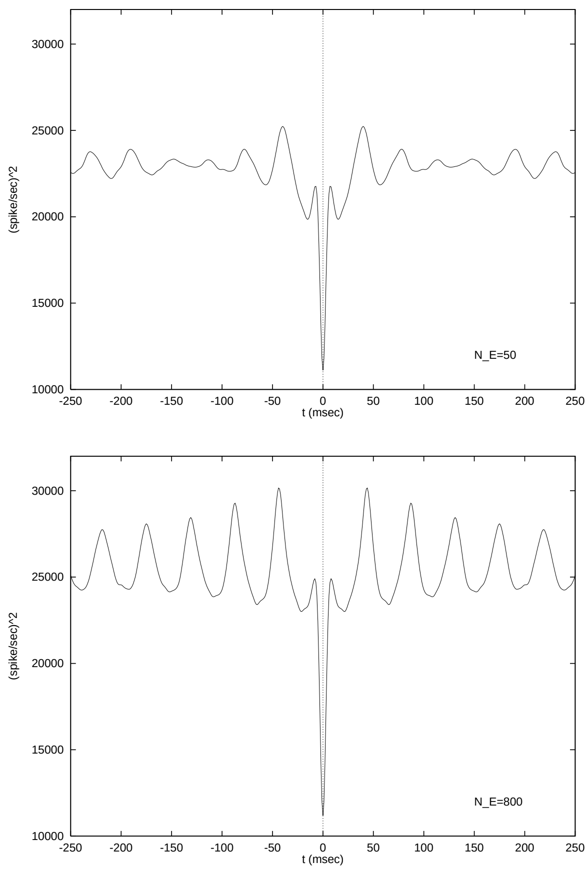

Figure 16: AC of a neuron with maximal activity in a synchronous oscillatory state for a network of $N_E = 50, N_I = 10$ neurons (upper graph) and for $N_E = 800, N_I = 160$ (lower graph). The ACs were calculated with spike trains of 36 sec long and they were smoothed with Gaussian filter of variance 3 $msec$.

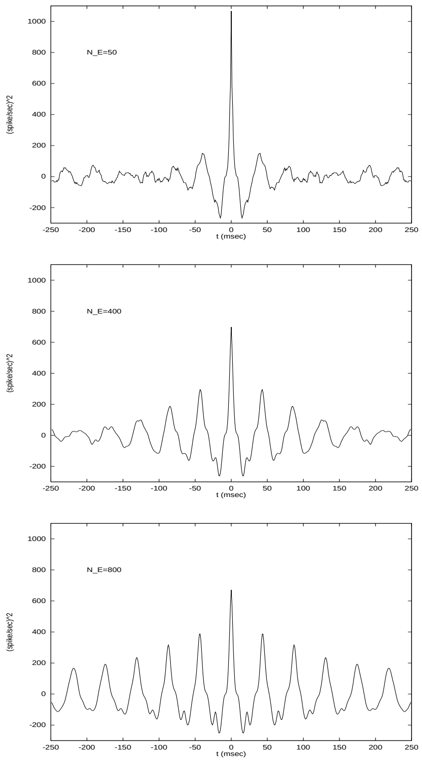

Figure 17: AC of the averaged instantaneous activity in the synchronous oscillatory state for $N_E = 50, N_I = 10$; $N_E = 400, N_I = 80$ and $N_E = 800, N_I = 160$. The AC was computed from the activity of the network during a period of 9 sec after stimulus onset.

of a neuron for $N_E = 50$.

This noise is synchronized across the network, as shown by the AC of the mean excitatory rate, Fig.18 A. However, inspection of the size dependence of the mean-rate of the excitatory population reveals that this variability is a finite size effect. As the network size increases it becomes more oscillatory. As is seen in Figures 17 B for the single neuron AC and in Fig. 18 B-C for the population activity, the oscillatory component of the dynamic remains synchronized at large N while the aperiodic component decreases in magnitude and probably vanishes at large N. According to the above classification this network is, therefore, in a synchronous oscillatory state.

Asynchronous states: In an asynchronous state the mean synaptic conductance of the neurons is almost constant in time. In our model neurons with constant conductances and external currents are almost always periodic. It is therefore rare to find

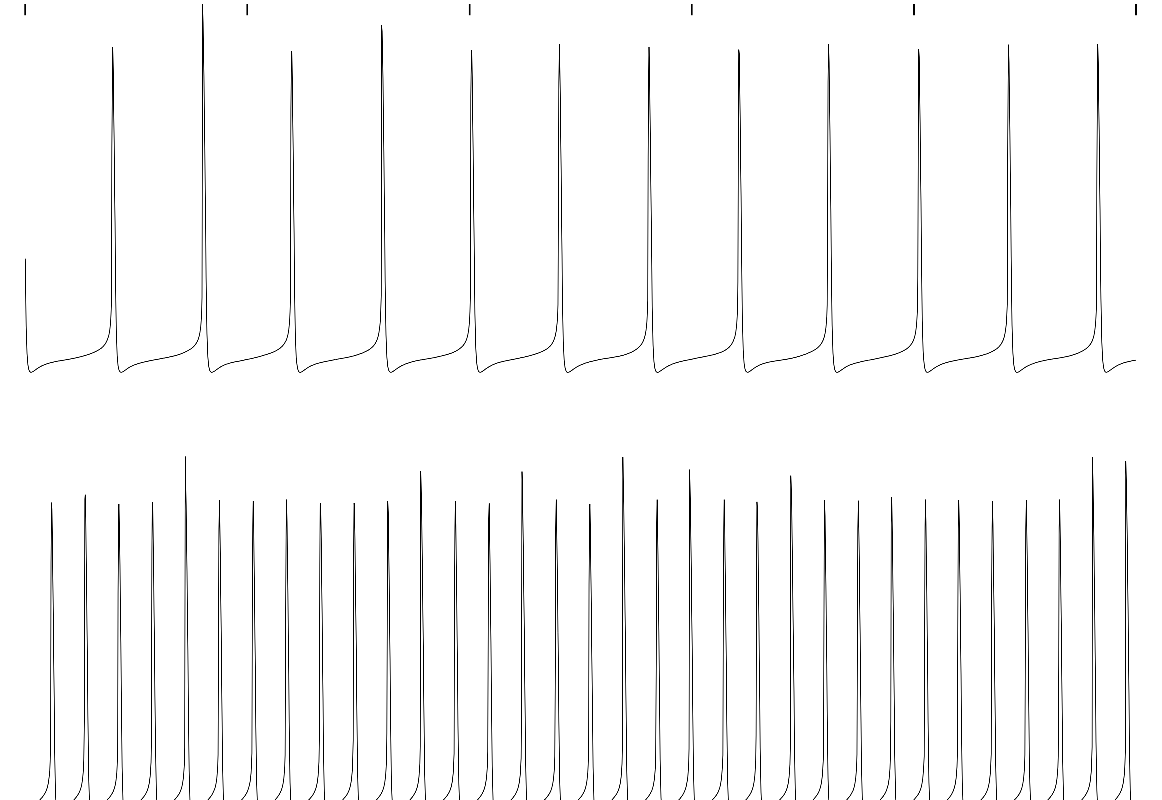

Figure 18: Membrane potential of two neurons in a network with $N_E = 800, N_I = 160$ in the A state (free of noise). The small fluctuations in the amplitude of the spikes are due to the fact that in this plot the spikes were not sampled at each time step.

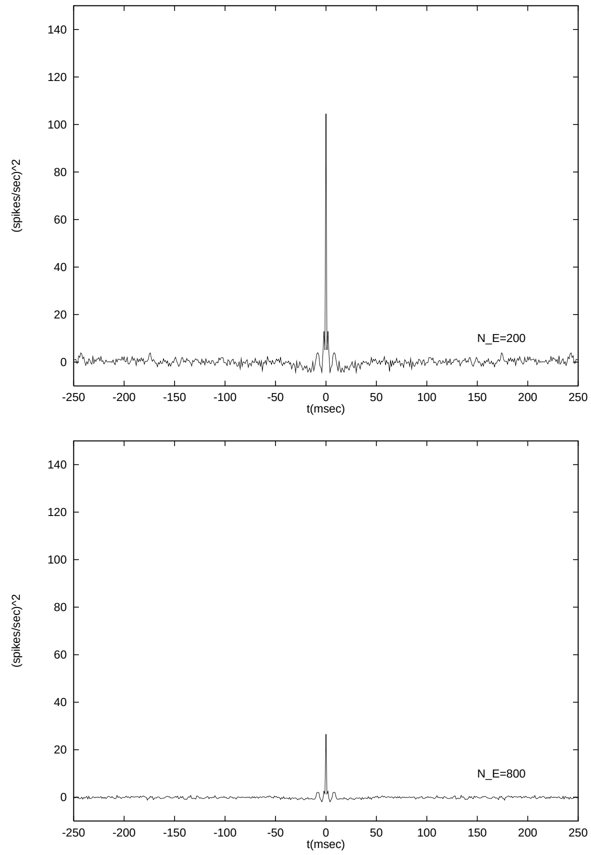

Figure 19: AC of the mean excitatory rate of the excitatory population for $N_E = 200, N_I = 40$ and $N_E = 800, N_I = 200$ in the SC state with local noise of large amplitude ($\sigma = 4\ \mu A/cm^2(msec)^{1/2}$). The AC was computed from the activity of the network recorded during 9 sec after the stimulus onset.

a state which is asynchronous but exhibits substantial degree of irregularity on a local level. Thus, asynchronous states in our model, with constant external currents, are characterized by a local periodic behavior. An example is a network with parameters similar to that of Fig.16-17 but with weaker synaptic conductances (for parameters see Table 1 of the Appendix). As shown in Fig.15, the variance of S_K in this case decreases to zero like $1/K$.

Another type of an asynchronous state occurs when a strong local noise is added. To study the effect of external noise, we have added uncorrelated stochastic currents to the neurons in the two populations (see Eq. (4) and the details in the Appendix). In the absence of this noise the network is in a SC state.

Fig. 19 shows the AC of the mean excitatory rate for $N_E = 200$ and $N_E = 800$ for large noise amplitude ($\sigma = 4\ \mu A/cm^2(msec)^{1/2}$). The amplitude of the AC decreases

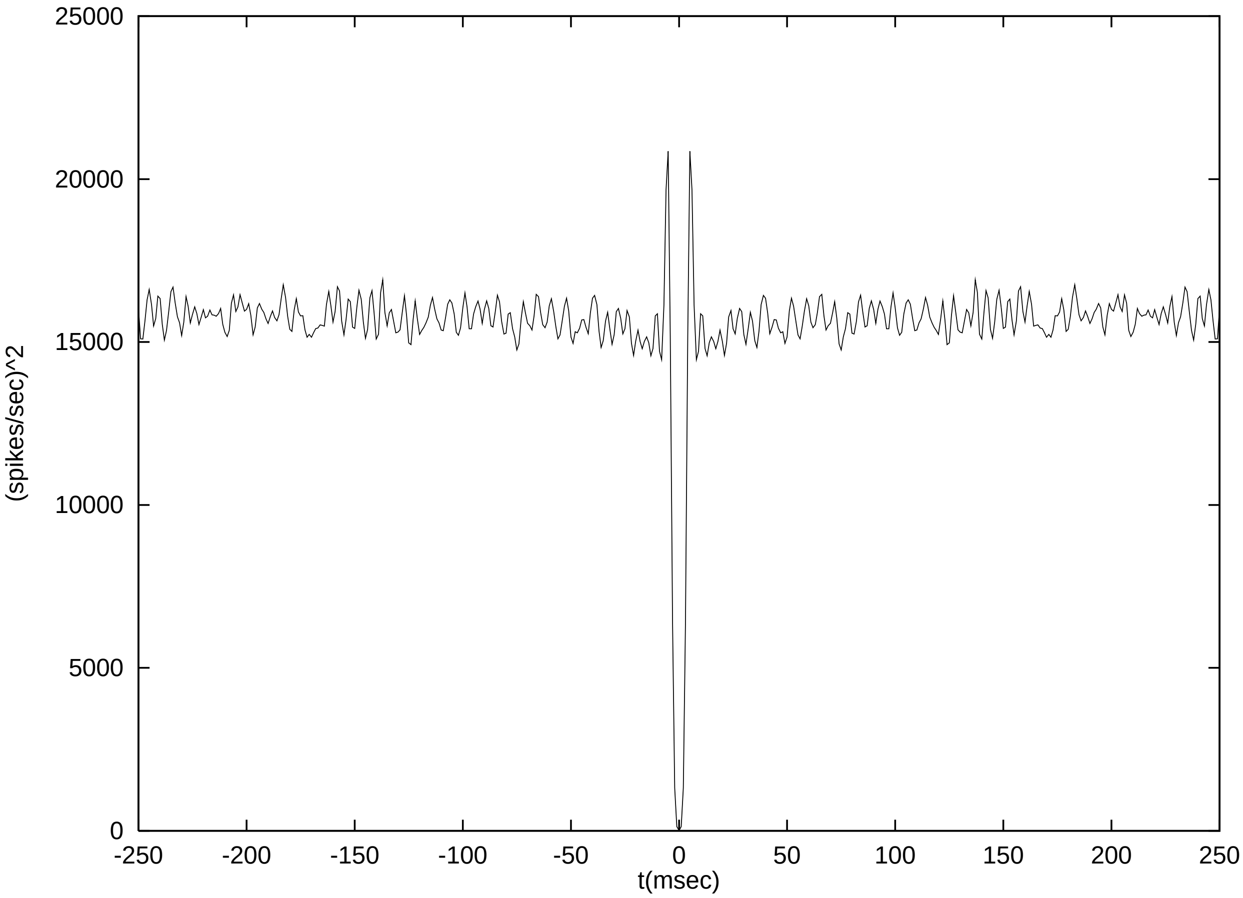

Figure 20: AC of a single neuron ($\theta = 0^{\circ}$) in the SC state with local noise of large amplitude ($\sigma = 4\ \mu A/cm^2(msec)^{1/2}$). $N_E = 800, N_I = 160$; the spike train was 9 sec long and the AC was smoothed with a Gaussian filter of window 1 $msec$.

by roughly a factor of 4 as the system size increases, suggesting to classify this state as asynchronous. This conclusion is confirmed by the analysis of the variance in the subpopulation activity, S_K, which decreases to zero as K increases (Fig. 15).

Unlike the previous asynchronous state case, in this case the AC of a single neuron decays fast even in the large system (Fig. 20) reflecting the action of the external local noise.

It is important to note that to destroy the synchrony of the state, the size of the local noise has to be bigger than a threshold value. Adding weaker noise will reduce the level of synchrony but will not destroy it.

To demonstrate this point, we present in Fig. 21 the AC of the mean excitatory rate for $N_E = 200,\ 800,\ 1600.$ for small noise amplitude ($\sigma = 2\ \mu A/cm^2(msec)^{1/2}$). The amplitude decreases with N but saturates at a nonzero value at large N, as shown quantitatively in Fig. 15. However, the level of synchrony in this case, as

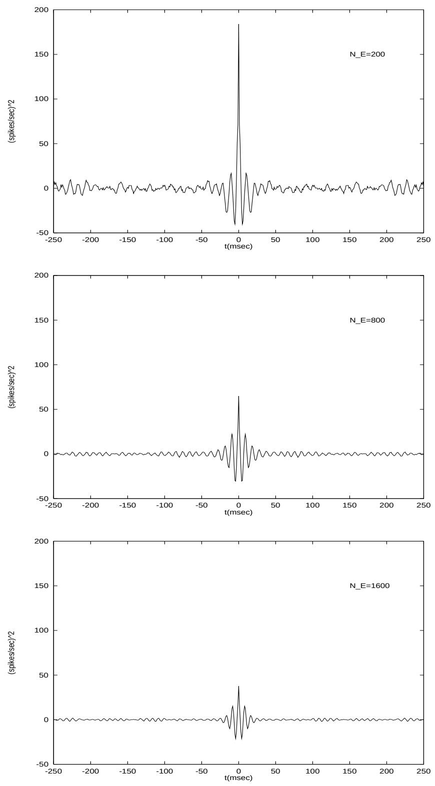

Figure 21: The AC of the mean excitatory activity of the excitatory population for increasing sizes of the network ($N_E = 200, N_I = 40,\ N_E = 800, N_I = 160$ and $N_E = 1600, N_I = 320$). The parameters of the network are those of the SC state. Local noise is added: $\sigma = 2\ \mu A/cm^2(msec)^{1/2}$. The ACs have been computed from the activity of the network during 9 sec after stimulus onset.

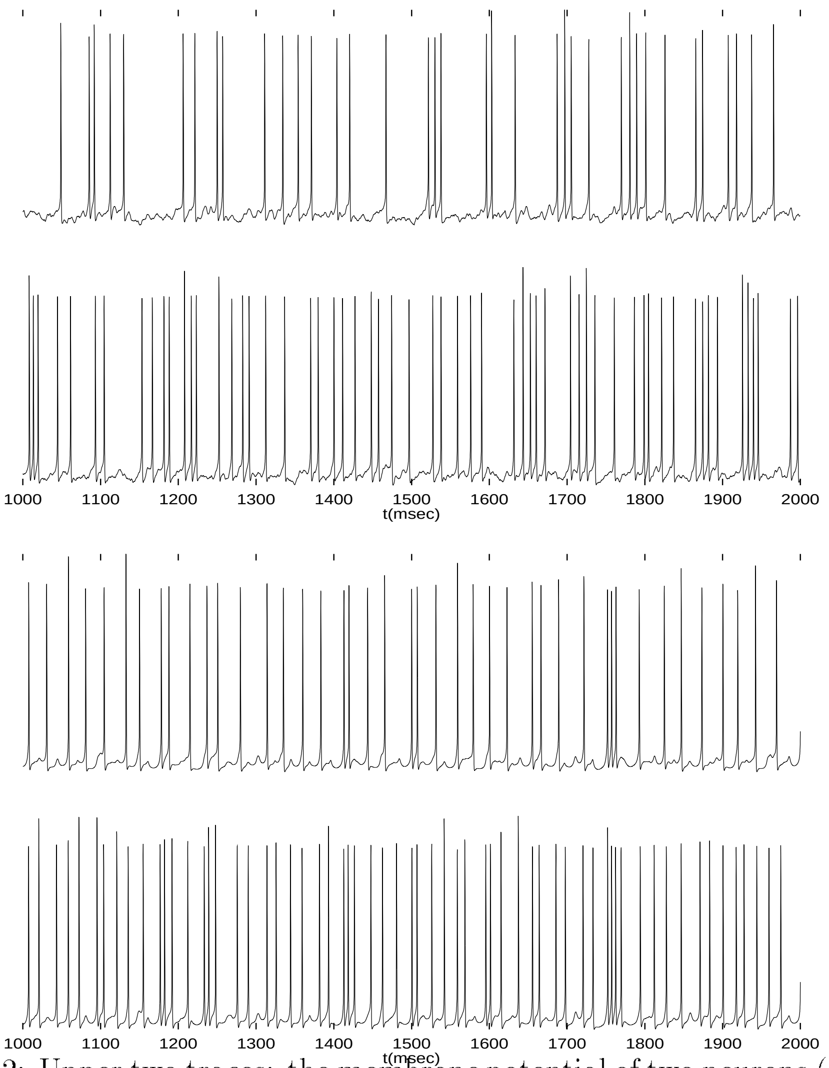

Figure 22: Upper two traces: the membrane potential of two neurons (POs $\theta = -20.7^o$ and $\theta = -17.1^o$) in the SC state with stochastic noise ($\sigma = 2\ \mu A/cm^2(msec)^{1/2}$). Lower two traces: the membrane potential the same neurons but in the SC state free of stochastic noise.

measured by the value 20 $(spikes/sec)^2$, of the variance of the subpopulation activity at large K (Fig. 15), is significantly lower than that of the system without noise, $\approx$ 400 $(spikes/sec)^2$ (Fig. 13), reflecting the reduction of synchrony by the local noise.

This is also seen in Fig. 22 (two upper traces) where the potentials of two neurons are shown as functions of time. The neurons are considerably noisier and less synchronized than in the system without noise (2 lower traces in Fig. 22).

6. Summary and Discussion

We have studied the properties of network models consisting of point neurons with conductance based dynamics. The network input and connectivity pattern mimics the gross architecture of a hypercolumn in primary visual cortex. We have focused on the issue of temporal irregularity and synchrony. A main finding of the present work is that for a reasonable parameter range the network exhibits a strongly irregular temporal behavior. One measure of this variability is the magnitude and form of the ACs of the activity of individual neurons. In fact, the ACs obtained in our model are comparable in size and shape to many ACs measured extracellularly in visual cortex during visual stimulation. In our model the dynamics was (in most of our studies) deterministic, free of stochastic noise, and with input currents that were constant in time. Hence the only source of variability is the noise generated by the strongly nonlinear internal dynamics of the network. In reality, both the internal dynamics and stochastic processes (such as stochastic synaptic release) as well as fluctuating synaptic input currents from outside the local network, are expected to contribute to the variability.

We have referred to the deterministic noise in our system as chaos. Establishing the chaotic nature of the dynamics requires demonstrating its sensitivity to the initial conditions. Specifically, one needs to show that two trajectories which start from slightly different initial conditions diverges exponentially fast with time.

Qualitatively our system exhibits sensitivity to the initial conditions when it is in the 'chaotic' state, as demonstrated in Fig. 23. As the figure shows, this sensitivity is absent in the oscillatory state. However, we have not yet established systematically that this sensitivity is indeed exponential.

The neurons in the model exhibit a strong tendency to fire in bursts although these bursts are highly irregular. This burstiness is a network property, since the isolated model neurons are spiking regularly. Another interesting feature of the temporal structure is that contrary to the naive expectations, we find that neurons with low firing rates are more oscillatory than neurons with high rates. Both the bursts and the damped oscillations are reminiscent of the activity of neurons in cat and monkey visual cortex [15, 41, 42]. However, we are not aware of experimental support for the prediction that oscillations are more pronounced in less optimally stimulated neurons.

Another main finding is the fact that the deterministic noise is strongly correlated across the network, a property which we termed 'synchronous chaos'. The synchronous nature of the network was demonstrated by the substantial CCs between neuronal pairs. The CCs usually exhibit a central peak with a width of about 10 $msec$. Many of them show additional structures, such as troughs and secondary peaks (see Fig. 5). It should be noted that the detailed structure of the CCs is rather sensitive to the size of the window used for smoothing, so detailed comparison with experimental results is difficult. Nevertheless, the time scales and the magnitudes of the CCs are in agreement with experimental results for the 'narrow' CCs observed in visual cortex for visually stimulated neurons with roughly the same range of firing rates as in our model [10]-[16] (The 'broad' CCs will be discussed below). An interesting feature of the model CCs is the fact that the central peaks of the CCs

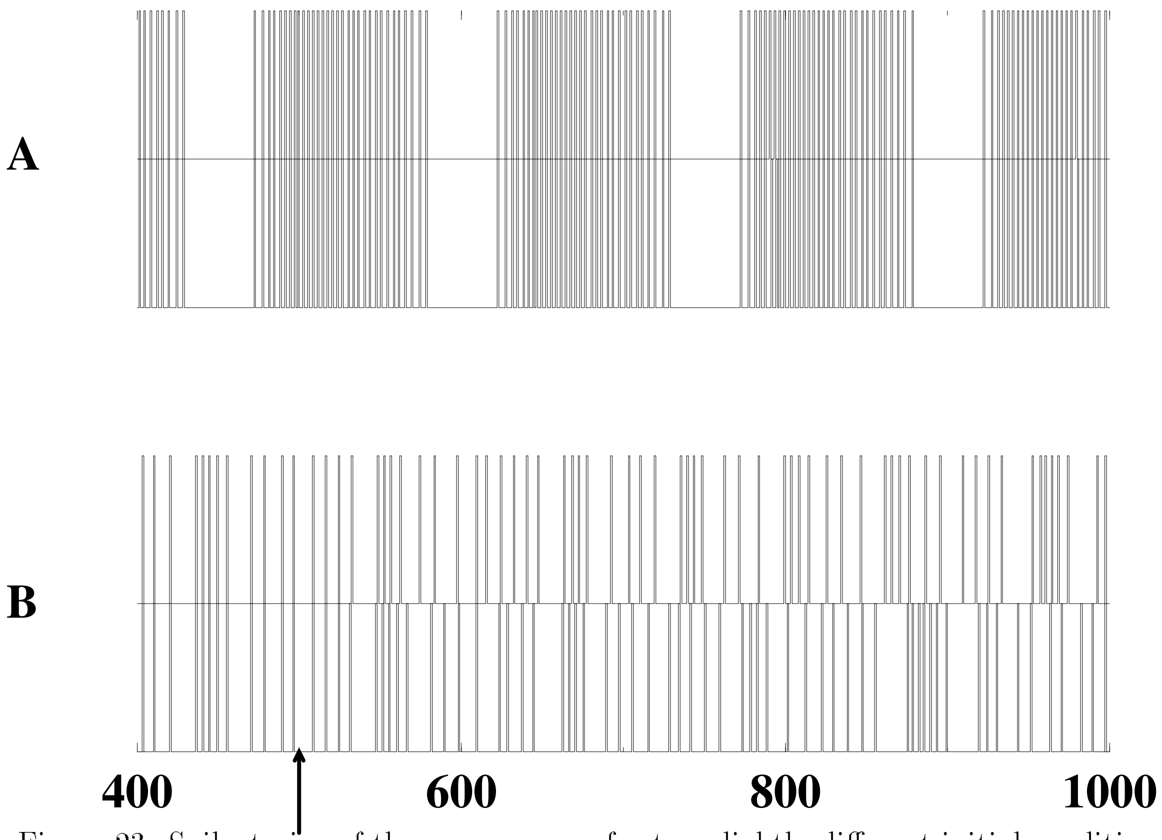

Figure 23: Spike trains of the same neuron for two slightly different initial conditions in the chaotic state. At $t = 500$ $msec$ a perturbation of 0.02 mV has been done on one neuron in the network all the other neurons remaining unperturbed. A: in the synchronous oscillatory state. B: in the SC state.

of neuronal pairs with different rates are shifted from zero delay (see Fig. 8). It is interesting to note that time shifts of the similar scales (few $msec$) have been recently reported for CCs in cat visual cortex [41, 43]. The observed variation of the phase shifts with the change in the stimulus orientation relative to the POs of the correlated pair is qualitatively consistent with the model predictions. A quantitative analysis of the CCs in our model and a detailed comparison with experimental data concerning amplitudes, widths, and phase shifts will be reported separately.

In our model the SC state is not a universal property. In large regions of the parameter space the network exhibited synchronized undamped oscillations. Asynchronous states are found in oscillatory regimes for relatively weak interactions or when sufficiently strong stochastic noise is injected to the system. It should be noted that asynchronous chaotic states where neuronal activities are strongly variable but only weakly correlated, are absent in our model as long as there is no stochastic noise and the external current is constant in time. This is because if the correlations are weak, the total synaptic current converging on each neuron is almost constant in time, and therefore elicits a regular response. Although it is impossible to define systematically the regions of parameters where chaos is observed, it is interesting to note that it is enhanced by the presence of inhibition. In our earlier work [24], we have found a SC state in a model of an excitatory network with dynamics which is similar to the present model. The main difference in the dynamics of the two models is in the synaptic time constants. In the previous model, synapses were assumed to act instantaneously. Further investigation of that model revealed that the chaotic state in the purely excitatory network is sensitive to the incorporation of synaptic time constants. Assuming a synaptic decay time constant as small as 0.5 $msec$ destroyed that phase and led instead to synchronized oscillations. Here we have found that including significant inhibitory feedback, yielded a robust chaotic state, which remains stable for synaptic decay constants of $5 - 10$ $msec$. Bush and Douglas [25] found that a common inhibitory input helps in stabilizing synchronized temporally irregular activity in a network of 7 excitatory and 1 inhibitory units. Our primary focus here is on mechanisms of synchrony and variability in large networks. The role of inhibition in synchronizing the activity in large networks has been recently investigated by several authors [44, 45, 46]. It has also been proposed that inhibition can amplify temporal fluctuations by canceling most of the excitatory input [9, 47, 48, 49]. It should be noted that our model does not incorporate this mechanism, as there is no approximate balance between the excitatory and inhibitory inputs.

We have studied the role of the network connections in shaping the orientation selectivity of the neurons. In the first range of parameters, the orientation tuning of the external inputs were sharp and the tuning was not directly affected by the cortical interactions, although they strongly affected the neuronal dynamics. Thus, in this parameter range, the network mimics the Hubel-Wiesel mechanism of orientation selectivity. We have found other parameter ranges where the network exhibits sharp orientation tuning even though the input tuning is very weak. In the extreme case where the input to all the neurons is the same, the network settles in a state where there is a 'hill' of activity peaked at arbitrarily chosen orientation column. We have found that the properties of the network are in full agreement with the predictions of the mean-field-theory which was recently developed in the framework of a much more simplified network dynamics [32]. It should be emphasized that in contrast to previous models [50], the cortical mechanism for orientation tuning studied here and in [32] does not rely on anisotropy of the cortical inhibitory connections. As demonstrated by the present work strong spatially modulated recurrent excitation, in conjunction with global inhibition, is sufficient. Enhancement of the orientation tuning by the recurrent lateral cortical connections has been also studied in a recent model of Somers *et al.* [51].

One predicted outcome of the cortical mechanism for orientation tuning is that the system will respond to a sudden change in the stimulus orientation by a moving activity profile, termed virtual rotation. We speculate that such a property might serve as a neural mechanism of the psychological phenomenon of mental rotation [52]. Transient changes in the population activity, which can be interpreted as a virtual rotation, have been observed in the monkey motor cortex [53]. Recently, a network model of a motion of the population activity profile which share similar features with our model has been proposed [54, 55]. In this model, however, the motion of the population activity profile is generated by an active modulation of synapses by external feedback signals. As far as we know, motion of the activity profile induced by changing the stimulus orientation has not been observed in primary visual cortex of behaving monkeys[56]. The experimental situation in cat cortex is not clear[57].

Of particular interest is the fact that in this range of parameters the CCs exhibit a broad component, the features of which depend on the stimulus orientation and the POs of the neuronal pair. This long-time component originates from a cooperative mode which corresponds to slow spontaneous fluctuations in the center of the activity profile of the population. Superimposed on this component is a narrow component which reflects the other internal modes of fluctuations which rapidly decay. It is interesting to note that this property agrees with the prediction of the mean field theory despite the fact that this theory assumed a network of stochastic neurons which are weakly correlated (i.e., the network is in an asynchronous state), whereas here the network is in a synchronized state.

The marginal phase was obtained in our model by reducing the adaptation current of the excitatory neurons. This is in accord with the mean field theory which predicts that for this phase to appear, the gain of the neuron must be larger than a critical value. A more systematic survey of the effects of varying the maximal conductance of the adaptation current has yet to be done.

In measurements of CCs in cortex, it is often observed that in addition to the above mentioned 'narrow' CCs, there are also 'broad' CCs with time scales of the order of a few hundred $msec$. These broad components may coexist with the narrow peak. The origin of these slow correlated fluctuations is not clear. The above results suggest that this property might originate from intrinsic cooperative spatio-temporal modes reflecting the slow wandering of the system between different collective states. A similar behavior has been found in the recent model of Usher *et al.* [26]. Concluding this issue, we have shown that the general architecture and dynamics of a 'cortical hypercolumn' is consistent with both the Hubel-Wiesel scenario in which the orientation tuning is dominated by the organization of the afferents and the scenario in which it is greatly enhanced by the local cortical interactions. In both cases, the network state is characterized by synchronized chaos. The main difference in their dynamics is in the temporal and spatial pattern of the CCs and the transient response to changing the stimulus orientation. Further experiments that will test the above predictions are needed in order establish the relative contributions of the two mechanisms in the various cortical areas that are selective for orientation.

Finally, we discuss to what extent we can make a quantitative comparison between our model and experiment. Throughout the present work, we focus on SC states defined as states that exhibit correlated, nonoscillatory temporal fluctuations that persist as the network size grows. In order to be able to scale up the system size N, it was necessary to scale the individual synaptic conductances by a factor of $1/N$, so that the total synaptic current remains finite, see Eq. (8). Therefore, in comparing the order of magnitude of the model parameters with the available data on cortical neurons and circuits, we have to consider the model at the scale which is relevant to cortex. To estimate the relevant scale of N we note that although the total number of anatomical synaptic contacts that input on a single pyramidal cell is on the order of $10^3 - 10^4$, the number of inputs that a neuron which is strongly activated by a stimulus receives from other neurons that are coactivated by the same stimulus is probably significantly smaller. A plausible assumption is that the number of such 'active inputs' is in the range of $10^2 - 10^3$. It is also plausible that about half of this input is coming from the local cortical region and the rest from remote areas in cortex or in thalamus.

The above estimated scale is comparable to our model network with $N \approx 2 \times 10^3$. For instance, for $N_E = 1600$, the excitatory neurons which are stimulated by near optimal orientation receive excitatory inputs from other 400 neurons in the network which are activated by the same stimulus. Using this value of N, the synaptic peak-conductance is $G_{EE} = 0.6 \times 10^{-3}\ mS/cm^2$ (see Table II and Eq. (8)). This will yield a single $EPSP$ with a peak value of about $0.2\ mV$, for our model neuron at rest. This synaptic strength is consistent with the available data from measurements of $EPSP$'s in cortical slices [58]. In addition, the magnitude of the time-independent external current I_0 to an optimally excited neuron is of the same order as the typical magnitude of the total synaptic current from the network. Thus, in our network, a neuron receives asynchronous inputs from several hundred 'external' synapses and roughly the same number of significantly synchronized inputs from the local circuit. Besides these inputs the neuron receives a few tens of synchronized inputs from local inhibitory neurons. We thus conclude that the SC state in our model network with $N = 1600$ yields a qualitatively plausible explanation for the variability and synchrony in cortical networks. It should be noted however that for most of the neurons the statistics of the temporal fluctuations shown in our simulations differ from Poisson statistics, as indicated by the shapes of the interspike interval histograms (see Fig. 6). In contrast, interspike interval histogram of cortical neurons often have a Poisson-type shape [8]. This difference may not be too significant, given the still simplified nature of the dynamic and architecture of the model.

An interesting issue which has been the subject of considerable debate is the mechanism that stabilizes neuronal activity in cortex in face of the numerous synaptic inputs that a pyramidal neuron receives [9]. Considering this issue, we note that the threshold potential in our model is 11 mV, and the external current I_0 of the optimally stimulated neurons is sufficient by itself to drive them above threshold. Nevertheless, the additional 400 inputs from synapses with 0.2 mV peak $EPSP$ do not drive the neurons to saturation. This stability is due to several factors. First, the negative inhibitory current partially offsets the excitatory current. In addition, the response to the synaptic current is considerably suppressed during the refractory periods of the neuron as well as when it is in a depolarized state where its time constant is reduced. This suppressive effect is amplified by the synchrony of the synaptic current [59, 60], and by the presence of strong A-current. Thus, our model shows that the input from the local cortical network may not affect much the average level of response in the system. Its main effect may be the modulation of the spatio-temporal pattern of activity, and possibly also the sharpening of the selectivity to the sensory stimuli.

Acknowledgements:

Fruitful discussions with M. Abeles, R. Ben-Yishai, D. Golomb, D. Kleinfeld, G. Mato, C. Meunier, R. Shapley, D. Tank, E. Vaadia are acknowledged. We also thank D. Golomb, G. Mato and C. Meunier for helpful comments on the manuscript. We are grateful to the two referees for their helpful comments. D.H. acknowledges the very warm hospitality of the Racah Institute of Physics and the Center for Neural Computation of the Hebrew University. We acknowledge the hospitality of the Marine Biological Laboratory, Woods Hole, during the summer of 1994, where part of the work was concluded. Most of the numerical simulations have been performed on the C90 of the IDRIS (Orsay, France). D.H. was supported in part by the PICS-CNRS (PIR Cognisciences and M.A.E) : “ Dynamique neuronale et codage de l'information: Aspects physiques et biologiques”. H.S. was supported in part by a grant of the

US-Israel Binational Science Foundation.

7. Appendix

In this appendix we present the details of the model, Eqs (1)-(4). Note that the sodium current and the potassium delayed rectifier have the same parameters as in the Hodgkin-Huxley model except for a shift of the membrane potential by 55 mV. This shift insures that the threshold to spike is in the range observed in cortical neurons. Membrane potential is measured in mV.

1. Sodium current: $I_{Na} = g_{Na} m^3 h (V - V_{Na})$.
   The inactivation variable h follows the first order relaxation equation:

$$\frac{dh}{dt} = \phi \frac{h_\infty(V) - h}{\tau_h(V)} \tag{13}$$

$$h_\infty(V) = \frac{a_h(V)}{a_h(V) + b_h(V)} \tag{14}$$

$$\tau_h(V) = \frac{1}{a_h(V) + b_h(V)} \tag{15}$$

$$a_h = 0.07 e^{(-(V+55)/20)} \tag{16}$$

$$b_h = 1/\left(1 + e^{(-(V+25)/10)}\right) \tag{17}$$

   In order to simplify the dynamics we consider that the activation variable m is fast and is equal to its instantaneous equilibrium value given by:

$$m_\infty(V) = \frac{a_m(V)}{a_m(V) + b_m(V)} \tag{18}$$

$$a_m(V) = 0.1 \frac{(V+30)}{1 - e^{(-(V+30)/10)}} \tag{19}$$

$$b_m(V) = 4 e^{(-(V+55)/18)} \tag{20}$$

   The factor ϕ has been introduced in order to tune the maximum firing rate to the desired high value. We use $\phi = 4$.

2. Delayed-rectifier potassium current: $I_K = g_K n^4 (V - V_K)$.
   The inactivation variable n satisfies:

$$\frac{dn}{dt} = \phi \frac{n_\infty(V) - n}{\tau_n(V)} \tag{21}$$

$$n_\infty(V) = \frac{a_n(V)}{a_n(V) + b_n(V)} \tag{22}$$

$$\tau_n(V) = \frac{1}{a_n(V) + b_n(V)} \tag{23}$$

$$a_n = 0.01 \frac{(v + 45)}{1 - e^{(-(V+45)/10)}} \tag{24}$$

$$b_n = 0.125 e^{(-(V+55)/80)} \tag{25}$$

3. A-current: $I_A = g_A ab(V - V_A)$

   We have assumed activation is instantaneous and satisfies:

$$a = a_\infty(V) = \frac{1}{1 + e^{(-(V+50)/4)}} \tag{26}$$

   The relaxation time of the inactivation variable is assumed to be independent of the membrane potential: $\tau_b = 10\ msec$ and the following relaxation equation has been used:

$$\frac{db}{dt} = \frac{b_\infty(V) - b}{\tau_b} \tag{27}$$

$$b_\infty = \frac{1}{1 + e^{((V+70)/2)}} \tag{28}$$

4. Persistent sodium current: $I_{NaP} = g_{NaP} s_\infty(V)(V - V_{Na})$.

   We have used the following expression for the activation variable:

$$s_\infty(V) = \frac{1}{1 + e^{(-0.3(V+50))}} \tag{29}$$

5. Slow potassium current: $I_z = g_z z(V - V_K)$.

   This current is incorporated into the dynamics of the excitatory population. The activation variable z satisfies the relaxation equation:

$$\frac{dz}{dt} = \frac{z_\infty(V) - z}{\tau_z} \tag{30}$$

   where $\tau_z = 60\ msec$ is independent of the membrane potential and

$$z_\infty(V) = \frac{1}{1 + e^{(-0.7(V+30))}} \tag{31}$$

6. Local noise: I_{noise}.

This noise is obtained by integrating the stochastic differential equation:

$$\frac{dI_{noise}}{dt} = -\frac{I_{noise}}{\tau_{noise}} + \eta(t) \tag{32}$$

where $\eta(t)$ is a number chosen at random in $[-\sigma, \sigma]$ and is not correlated in time. In all our simulations in which local noise is added $\tau_{noise} = 5\ msec$.

References

1. Noda, H. and Adey, W.R. Firing variability in cat association cortex during sleep and wakefulness. *Brain Research*, 18:513-526, 1970.
2. Burns, B.D. and Webb, A.C. The spontaneous activity of neurons in the cat's cerebral cortex. *Proc. R. Soc. Lond. B* 194:211-213, 1976.
3. Schiller, P.H., Finlay, B.L., and Volmann, S.F. Short-term response variability of monkey striate neurons. *Brain. Res.*, 105:347-349, 1976.
4. Dean, A.F. The variability of discharge of simple cells in cat striate cortex. *Exp. Brain Res.*, 44:437-440, 1981.
5. Tolhurst, D.J., Movshon, J.A., and Dean, A.F. The statistical reliability of signals in single neurons in cat and monkey visual cortex. *Vision Res.* 23:775-786, 1983.
6. Vogels, R., Spileers, W., and Orban, G.A. The response variability of striate cortical neurons in the behaving monkey. *Exp. Brain. Res.*, 77:432-436, 1989.
7. Connors, B.W., Gutnick M.J., and Prince, D.A. Electrophysiological properties of neocortical neurons in vitro. *J. Neurophysiol.*, 48:1302-1320, 1982.
8. Softky, W. and Koch, C. The highly irregular firing of cortical cells is inconsistent with temporal integration of random EPSP's. *J. Neurosc.* 13:334-350, 1993.
9. Shadlen, M.N., Newsome W.T. Noise, neural codes and cortical organization. *Current Opinion in Neurobiol.* 4:569-579, 1994.
10. Ts'o, D.Y., Gilbert, C.D. and Wiesel T.N. Relationship between horizontal interactions and functional architecture in cat striate cortex as revealed by cross-correlation analysis. *J. Neurophysiol.* 6:1160-1170, 1986.
11. Krüger, J. and Aiple, F. Multimicroelectrode investigation of monkey striate cortex: spike train correlations in the infragranular layers. *J. Neurophysiol.* 60:798-827, 1988.
12. Gochin, P.M., Miller, E.K., Gross, C.G., and Gerstein, G.L. Functional interactions among neurons in inferior temporal cortex of the awake macaque. *Exp. Brain. Res*, 84:505-516, 1991.
13. Fetz, E., Toyama, K., and Smith,W. Synaptic interactions between cortical neurons. In Cerebral Cortex. Peters, A. and Jones, E.G. (Eds.) 9:1-80. Plenum Press, New York, 1991.
14. Nowak, L.G., Munk, M.H.J., Nelson, J.I., James, A.C., Bullier, J. The structural basis of cortical synchronization. I. Three types of interhemispheric coupling. preprint; The structural basis of cortical synchronization. II. Effects of cortical lesions. preprint.
15. Gray, C.M., König, P., Engel, A.K. and Singer, W. Oscillatory responses in

cat visual cortex exhibit intercolumnar synchronization which reflects global stimulus properties. *Nature* 338:334-337, 1989.

16. Eckhorn, R., Reitboeck, H.J., Arndt, M. and Dicke, P. Feature linking among distributed assemblies: Simulations and results from cat visual cortex. *Neural Computation* 2:292-306, 1990.
17. Engel, A.K., Konig, P., Kreiter, A.K. and Singer, W. Interhemispheric synchronization of oscillatory neuronal responses in cat visual cortex. *Science* 252:1177-1180, 1991.
18. Fregnac, Y. Bringuier, V., and Baranyi, A. Oscillatory neuronal activity in visual cortex: a critical re-evaluation. In Temporal Coding in the Brain: Research and Perspectives in Neurosciences, Buzsaki, G. Llinas R., Singer, W., Berthoz, A., and Christen Y. (Eds.) Springer-Verlag, Berlin, 1994.
19. Hubel, D.H. and Wiesel, T.N. Receptive fields, binocular interaction and functional architecture in the cat's visual cortex. *J. Physiol. Lond* 160:106-154, 1962.
20. Bergé, P., Pomeau, Y. and Vidal, C. Order within Chaos: Towards a Deterministic Approach to Turbulence. Johny Wiley and Hermann, Paris, 1984.
21. Ginzburg, I., and Sompolinsky, H. Theory of correlations in stochastic neural networks. *Phys.Rev.E* 50:3171-3191, 1994.
22. Abeles, M., Corticonics: Neural Circuits of the Cerebral Cortex. Cambridge University Press, Cambridge, 1991.
23. Hodgkin, A.L., and Huxley, A.F. A quantitative description of membrane current and its application to conduction and excitation in nerve. *J. Physiol. (London)* 117:500-544, 1952.
24. Hansel, D., and Sompolinsky, H. Synchronization and computation in a chaotic neural network. *Phys. Rev. Lett.*, **68**, 718-721, 1992.
25. Bush P., and Douglas R., Synchronization of bursting action potential discharge in a model network of neocortical neurons. *Neural Computation*, 3:19-30, 1991.
26. Usher, M., Stemmler, M., Koch, C. and Olami, Z. Network amplification of local fluctuations causes high spike rate variability, fractal firing patterns and oscillatory local field potentials. *Neural Computation* 6:795-836, 1994.
27. Tsumoto, T., Eckart, W., Creutzfeldt, O.D. Modification of orientation sensitivity of cat visual cirtex neurons by removal of GABA-mediated inhibition. *Exp. Brain Res.* 34:351-363, 1979.
28. Sillito, A.M., Kemp, J.A., Milson, J.A. and Berardi, N. A re-evaluation of the mechanisms underlying simple cell orientation selectivity. *Brain Res.* 194:517-520, 1980.
29. Chapman, B., Zahs, K.R., and Stryker, M.P. Relation of cortical cell orientation selectivity to alignment of receptive fields of the geniculocortical afferents that arborize within a single orientation column in ferret visual cortex. *J.*

Neurosci. 11:1347-1358, 1991.

30. Martin, K.A.C. From single cells to simple circuits in the cerebral cortex. *Q. J. Exp. Physiol.* 73:637-702, 1988.
31. Douglas, R.J., Mahowald, M.A. and Martin, K.A.C. Hybrid analog-digital architectures for neuromorphic systems. Preprint, 1994.
32. Ben-Yishai, R., Lev Bar-Or, R. and Sompolinsky, H. Theory of orientation tuning in visual cortex. Proc. Natl. Acad. Sci. (USA), in press (1994).
33. Anderson, P. W. and Stein D. L. Broken symmetry, emergent properties, dissipative structures, life and its origin: are they related? In Self-Organizing Systems: The Emergence of Order, Yates F.E. (Ed.) Plenum Press, New York, 1984.
34. The term *marginal phase* refers to the fact that when the input is isotropic, each of the spatially inhomogeneous states of the network is dynamically stable to all perturbations, except those that induce transitions between these states.
35. Connor, J.A., Walter, D., and McKown, R. Neural repetitive firing: modifications of the Hodgkin-Huxley axon suggested by experimental results from crustacean axons. *Biophys. J.* 18:81-102.
36. Rush, M.E., and Rinzel, J. The potassium A-current, low firing rates and rebound excitation in Hodgkin-Huxley models. Preprint, 1994.
37. Llinas, R.R. The intrinsic electrophysiological properties of mammalian neurons: insights into central nervous system function. *Science* 242:1654-1664, 1988.
38. Stafstrom, C.E., Schwindt, P.C., and Crill, W.E Negative slope conductance due to a persistent subthreshold sodium current in cat neocortical neurons in vitro. *Brain Research* 236:221-226, 1982.
39. Gustafsson, B., Galvan, M., Grafe, P. and Wigstrom, H. Transient outward current in mammalian central neuron blocked by 4-aminopyridine. *Nature* 299:252-254, 1982.
40. Storm, J.F., Functional diversity of K^+ currents in hippocampal pyramidal neurons. *Seminars in THE NEUROSCIENCES* 5:79-92, 1993.
41. Freiwald, W. Dynamik lokaler synchronisationen: eine elektrophysiologische untersuchung mit stereotetroden im visuellen system der säugetiere, Diplomarbeit, Tubingen, 1993.
42. Bair, W., Koch, C., Newsome, W., and Britten, K. Power spectrum analysis of bursting cells in Area MT in the behaving monkey. *J. Neurosc.* 14:2870-2892, 1994.
43. König, P., Engel, A.K., Roelfsema, P.R., and Singer, W. How precise is neuronal synchronization. *Neural Comp.* 7:469-486, 1995.
44. Van Vreeswijk, C., Abbott, L.F. and Ermentrout, G.B. Inhibition, not excitation synchronizes coupled neurons. *J. Comp. Neurosci.* 1:313-321, 1995.
45. Hansel, D., Mato, G. and Meunier, C. Synchrony in Excitatory Neural Net-

works. *Neural Comp.* 7:307-337, 1995.
46. Ernst, U., Pawelzik, K. and Geisel, T. Synchronization induced by temporal delays in pulse coupled oscillators. *Phys. Rev. Lett.*, 74:1570-1573, 1995.
47. Tsodyks M., and Sejnowski, T. Rapid state switching in balanced cortical network models. Submitted to network (october 1994).
48. Amit D.J., and Brunel, N. Global spontaneous activity and local structured (learned) delay activity in cortex. Preprint, 1995.
49. Van Vreeswijk, C. and Sompolinsky, H. Theory of Randomly Connected Networks with Excitation-Inhibition Balance, Abstract in *Cortical Dynamics*, Jerusalem, 1995.
50. Woergotter, F. and Koch, C. A detailed model of the primary visual pathway in the cat: Comparison of afferent excitatory and intracortical inhibitory connection schemes for orientation selectivity. *J. Neurosc.* 11:1959-1979, 1991.
51. Somers, D. C., Nelson, S. B., and Sur, M. An emergent model of orientation selectivity in cat visual cortical simple cells. *J. Neurosc.*, in press., 1995.
52. Shepard, R.N. and Metzler, J. Mental rotation of three-dimensional objects. *Science* 171:701-703, 1971.
53. Georgopoulos, A.P., Lurito, J.T., Petrides, M., Schwartz, A.B., and Massey, J.T. Mental rotation of the neuronal population vector. *Science* 243:234-236, 1989.
54. Georgopoulos, A.P., Taira, M., and Lukashin, A. Cognitive neurophysiology of the motor cortex. *Science* 260:47-52, 1993.
55. Lukashin, A.V. and Georgopoulos, A.P. Directional operations in the motor cortex modeled by a neural network of spiking neurons. *Biol. Cybern.* 71:79-85, 1994.
56. Celebrini, S., Thorpe, S., Trotter, Y., and Imbert, M. *Visual Neurosc.* 10:811-825, 1993.
57. Shevelev, I.A., Sharaev, G.A., Lazareva, N.A., Novikova, R.V. and Tikhomirov, A.S. Dynamics of orientation tuning in the cat striate cortex neurons. *Neuroscience* 56:865-876,1993.
58. Mason, A., Nicoll, A., and Stratford, K. Synaptic transmission between individual pyramidal neurons of the rat visual cortex *in vitro*. *J. Neurosc.* 11:72-84, 1991.
59. Bernander, Ö, Koch, C., and Usher, M. The effect of synchronized inputs at the single neuron level. *Neural Comp.* 6:622-641, 1994.
60. Murthy, V.N., and Fetz, E.E., Effects of input synchrony on the firing rate of a three-conductance cortical neuron model. *Neural Comp.* 6:1111-1126, 1994.

Abbreviations

- Lateral geniculate nucleus: LGN
- Preferred orientation: PO
- Auto-correlation: AC
- Cross-correlation: CC
- Synchronous chaotic: SC

Table I

	E	I
C	1	1
g_{Na}	120	120
g_K	10	20
g_A	60	40
g_{NaP}	0.5	0.2
g_l	0.1	0.1
g_z	10	0
V_{Na}	55	55
V_K	-70	-70
V_A	-75	-75
V_l	-80	-80

Table II

	SC	SO	AS
τ_1^e	3	0.6	3
τ_2^e	1	0.2	1
τ_1^i	7	7	7
τ_2^i	1	1	1
g_{EE}	1	2.75	0.1
g_{IE}	2	1	0.1
g_{II}	1	1	0.1
g_{EI}	0.6	0.25	0.1
V_{syn}^e	0	0	0
V_{syn}^i	-75	-75	-75

Table Captions

Table I The values of the capacitance (in $\mu F/cm^2$), of the maximal ionic conductances (in mS/cm^2) and of the reversal potentials (in mV). The notations are defined in the Appendix.

Table II The synaptic parameters used in the simulations. SC: Synchronous Chaotic state; SO: Synchronous Oscillatory states; AS: Asynchronous state (without noise). Conductances in mS/cm^2, times in $msec$, reversal potentials in mV). The notations are defined in the Appendix.